A Laser Flash Photolysis Study of the Intramolecular Photoisomerization and Reduction of Dibenzo-*p*-dioxins

by

Ryan Roe Sasaki
B.Sc., University of Prince Edward Island, 1999

A Thesis Submitted in Partial Fulfillment of the
Requirements for the Degree of

Master of Science

In the Department of Chemistry

We accept this Thesis as conforming
to the required standard

[redacted]

Dr. P. C. Wan, Supervisor (Department of Chemistry)

[redacted]

Dr. M. B. Hocking, Department Member (Department of Chemistry)

[redacted]

Dr. N. Sherwood, Outside Member (Department of Biology)

[redacted]

Dr. A. Amiri (Hydroxyl Systems Inc.)

University of Victoria

Supervisor: Dr. P. C. Wan

Abstract

The mechanistic details of the photoisomerization and reduction of four dibenzo-*p*-dioxins **33, 39, 40** and **41** are reported. The dibenzo-*p*-dioxin ring system is common to chlorinated dioxins, which are known to be some of the most toxic compounds ever synthesized. Although chlorinated dioxins have dechlorination (typically via C-Cl bond homolysis) as an important photochemical reaction channel, we have recently shown that photoisomerization of the dibenzo-*p*-dioxin ring system is a significant reaction channel. Therefore, the kinetic details of the photoisomerization and subsequent reaction of the 2,2'-biphenylquinones would add further insight into the photochemical reactivity of these compounds. For this purpose, laser flash photolysis and conventional kinetic measurements are used to study the parent compound **33** and three derivatives, **39, 40** and **41**. It is shown that laser flash photolysis is able to kinetically resolve the growth of the 2,2'-biphenylquinone from its assumed spiroketone precursor, whereas the reduction of the 2,2'-biphenylquinone can be followed conveniently by UV-Vis spectrophotometry. The effects of pH have shown an acid catalysed effect on both the formation and disappearance of the 2,2'-biphenylquinones. Studies in different solvents and solvent isotope effects have illustrated the solvent participation in the reduction of the 2,2'-biphenylquinones. Electron-donating substituents has been shown to decrease the lifetimes of both the spiroketone and the biphenylquinone. The results of this thesis support a mechanism for the photochemical degradation of dibenzo-*p*-dioxins.

Examiners:

[redacted]

Dr. P. C. Wan, Supervisor (Department of Chemistry)

[redacted]

Dr. M. B. Hocking, Department Member (Department of Chemistry)

[redacted]

Dr. N. Sherwood, Outside Member (Department of Biology)

[redacted]

Dr. A. Amiri (Hydroxyl Systems Inc.)

TABLE OF CONTENTS

List of Tables

List of Figures

Acknowledgements

I would like to thank Dr. Peter Wan for his patience and understanding as a supervisor and for his ideas and guidance, throughout the last two years. I would also like to thank my friends from the Wan group, James Morrison, Kaya Forest, Sierra Rayne, Musheng Xu, Matt Lukeman, Devin Mitchell, Mitch Flegel, Darryl Brousmiche and John Cole for their support, both in and out of the University. I would also like to thank Dr. Cornelia Bohne and Luis Netter for their patience and tutelage on the laser system. Thanks as well to Chris Greenwood and David McGilivray for their assistance with NMR and mass spectroscopy, respectively. I am also extremely grateful to Aynsley and Layla for their huge commitment and support throughout the last couple of years. I would finally like to acknowledge UVic for funding and all the members of the Chemistry Department for their support.

Dedication

For Aynsley and Layla

Chapter 1

Introduction

Photochemical reactions are essential to life on Earth. For example, photochemistry is responsible for the synthesis of carbohydrates in green plants through the reduction of carbon dioxide by water using solar energy. Since the emergence of mechanistic organic chemistry in the 1960's, many new photoreactions have been discovered and utilized as synthetic tools. A large part of the field has intensely studied the photochemical reactions involving different functional groups, with a large emphasis placed on carbonyls, alkenes and aromatic compounds. While many photoreactions have been discovered in the last few years, the mechanistic aspects of organic photochemistry remain a huge obstacle.

The invention of highly sophisticated techniques have provided enormous insight into the field of mechanistic photochemistry. Tools such as laser flash photolysis, UV-visible spectroscopy, ESR, time-resolved-fluorescence and infra-red spectroscopy have provided a strong foundation in an effort to delineate the details of mechanistic photochemistry.

Photochemical reactions have the potential to react via two different paths. When a molecule is excited it can undergo chemical change within itself (unimolecular process), or it can react with another molecule (bimolecular process). These processes can be derived from both ionic and radical reactions. Ionic reactions are those in which covalent bonds are broken heterolytically, yielding charged species that can serve as reactants, intermediates or products. The other category of reactions are those in which

covalent bonds are broken homolytically, producing intermediates that possess unpaired electrons, and are called radicals. This thesis will focus on unimolecular photoreactions while a large emphasis will be placed on radical reactions resulting from bond homolysis. The intention of this introduction is to provide a brief overview on the photochemistry of several organic compounds that are relevant to this body of work. A small section covering the photodecomposition of environmentally relevant compounds will also be presented to emphasize the applications of this research.

1.1 Diaryl Ether Photochemistry

Photochemical reactions of diaryl ethers involve several different pathways for reaction. Eq. 1.1 shows homolytic cleavage of the C-O bond resulting in the formation of a phenyl radical and a phenoxyl radical.[1] The formed radicals are held in a solvent cage and can rearrange via an intramolecular process to give ortho and/or para substituted phenols. Another option involves the escape of the radicals from the cage, which upon hydrogen abstraction, will result in the corresponding benzene and phenol products. Aromatic substituents have been shown to influence this primary cleavage step. Another reaction of diaryl ethers involves photocyclization to yield dibenzofuran.[2,3] This reaction requires the presence of a labile ortho substituent so it can undergo eliminative photocyclization. In addition, ring closed diaryl ethers have shown intramolecular rearrangement when photolyzed.[4] All of these reactions will be explained in detail in the following sections.

1.1.1 Cleavage and Rearrangement

In 1952 Kharasch et al.[5] reported the photochemically induced cleavage and rearrangement of diaryl ethers. Their results, along with the findings of Bach and Barclay[6], demonstrated that irradiation of diphenyl ether (**1**) yielded unsubstituted phenol (**2**) along with the ortho and para substituted phenols **3** and **4**, respectively (Eq. 1.1). The intramolecularity of this rearrangement was proposed when no cross-products were detected in the photolysis of equivalent amounts of diphenyl ether (**1**) and bis(*p*-methylphenyl)ether (**5**) in alcohol (Eq. 1.2). Further testing of this reaction in a variety

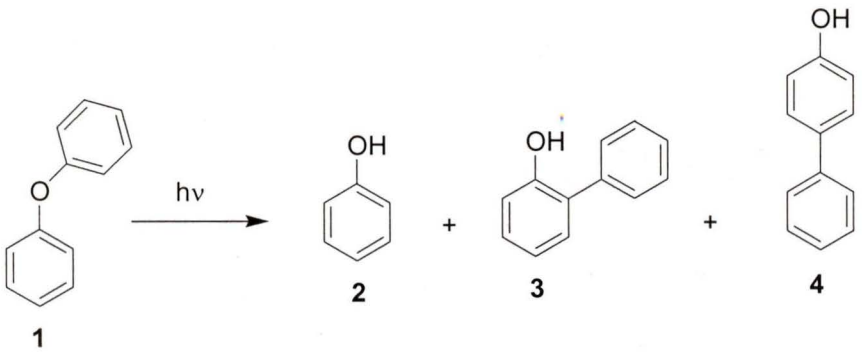

(1.1)

of solvents led to the conclusion that the rearrangement products observed were solvent dependent.[7] An observed decrease in the ratio of rearranged products to phenol upon photolysis of **1** in ether as opposed to isopropanol suggested that the decrease in solvent viscosity would allow for a more rapid escape of the caged radicals.

Other solvent studies revealed that the rearrangement was favoured in more polar solvents. This was explained by the stabilization of the quinoid intermediates in the rearrangement reaction through hydrogen bonding by the polar solvent. This stabilization would not be expected in non-polar solvents.

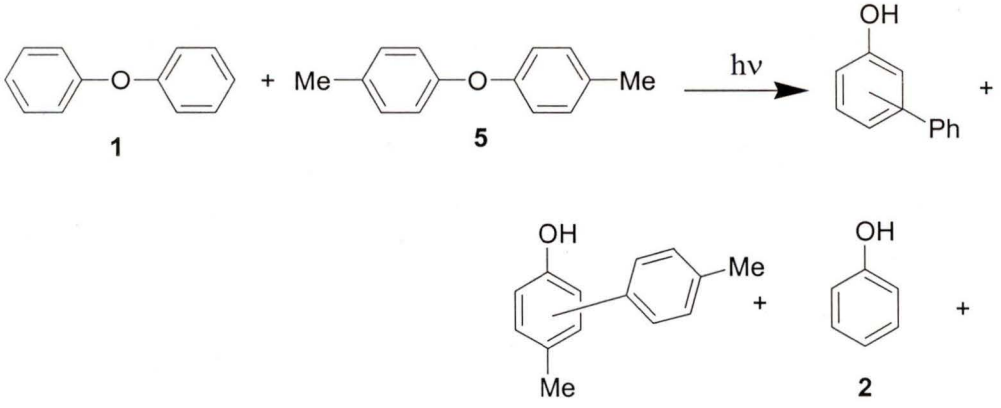

(1.2)

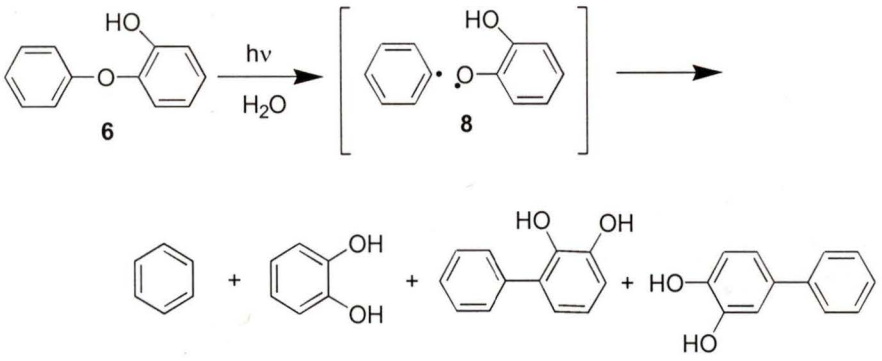

(1.3)

Joschek and Miller[8] have shown that photolytic cleavage of the aryl-O bond for 2 and 4-phenoxyphenol (**6** and **7**, respectively) is highly regioselective. The presence of the hydroxy- substituent on the ring influences cleavage to yield both the ortho and para phenoxy radicals **8** and **9**, respectively, as opposed to the unsubstituted phenoxy radical. The higher stability of the substituted phenoxy radicals formed governs the homolytic cleavage of the diphenyl ether in this case (Eq. 1.3 and 1.4). The substituent effects on the regioselectivity of the C-O bond fission was further investigated by Haga and Takayanagi.[9] Their work revealed that phenyl systems bearing electron-donating substituents favoured aryloxy-phenyl cleavage in contrast to those with electron withdrawing substituents (Scheme 1.1). The substituted diphenyl ether (**10**) can cleave via two different paths, a or b.

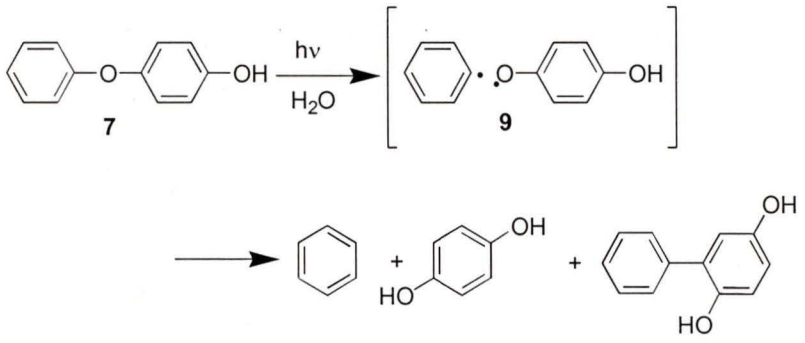

(1.4)

The results revealed that cleavage occurred via path a when the substituent is electron-donating (labelled X) while path b is the preferred mode for the ether with electron-withdrawing substituents (labelled X). Unexplainable results were obtained when p-fluoro substituted diphenyl ethers favoured path a despite the electron-withdrawing effects of this substituent.

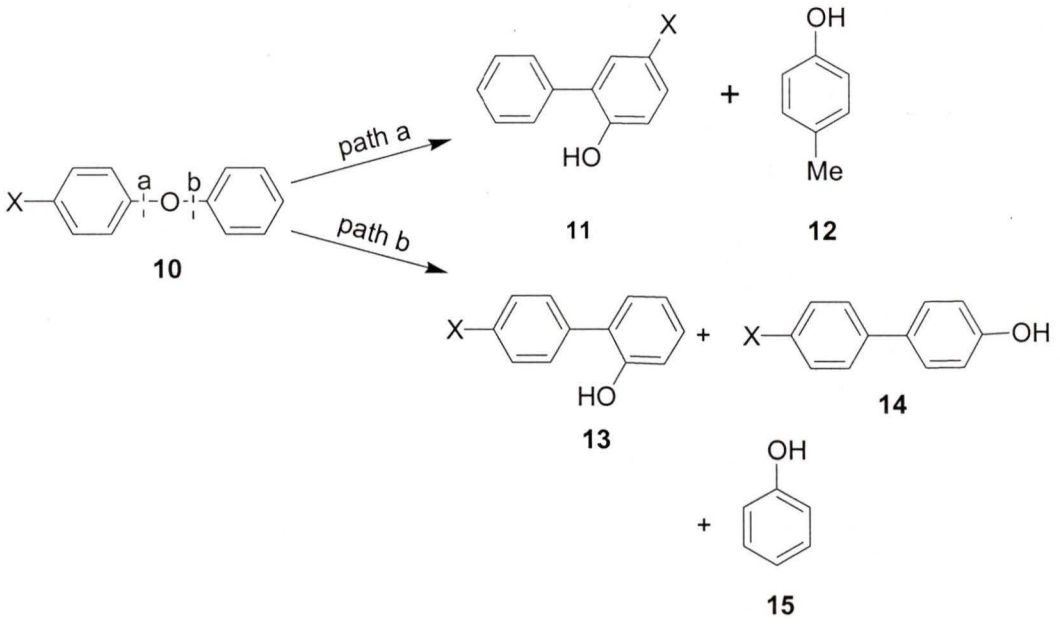

Scheme 1.1

1.1.2 Electrocyclic Ring Closure

Upon irradiation, diphenyl ethers with a photolabile group ortho to the ether linkage can undergo ring formation to form dibenzofurans. Low yields of dibenzofuran have been observed via irradiation of ethers of the type **16,** with a methoxy-substituent ortho to the ether linkage (Eq. 1.5).[10] Electron redistribution leads to stable dibenzofurans and the subsequent loss of methanol ensures an irreversible reaction.

Greater yields (45%) have been shown for **17** which has a chloro substituent in the ortho position (Eq. 1.6).[10] This reaction likely proceeds through an ylide intermediate that is directed by the labile substituent in the ortho position. Electrocyclization is the dominant photochemical pathway if there is a good leaving group in the ortho position. On the other hand, in the absence of a good leaving group, cleavage and rearrangement is the dominating avenue.

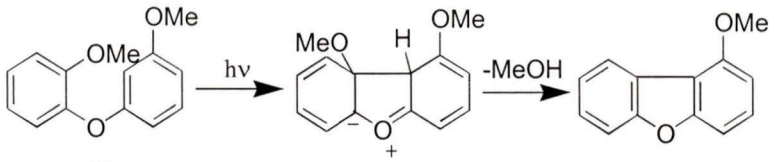

16 (1.5)

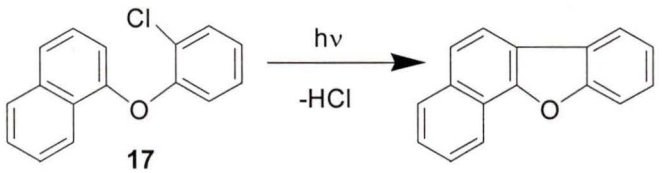

17 (1.6)

1.1.3 Intramolecular Rearrangement

Intramolecular rearrangements have been shown in diphenyl ethers that are joined by a carbon chain. The photoisomerization of xanthene (**18**) is one such example (Scheme 1.2).[4] Upon photolysis of **18**, biradical **19** is formed via singlet state aryl-O bond homolysis. The biradical may revert back to starting material or bond at the ortho-position of the phenoxy moiety to form the spiroketone **20.** The resulting spiroketone

may ring-open to yield the biphenyl *o*-quinone methide **21**. Once **21** is formed it can cackles to give the pyrans **22** or it can be trapped by water to yield **23**. The proposed reactive intermediates **19**, **20** and **21** have not been directly observed to date, presumably due to their very short lifetimes.

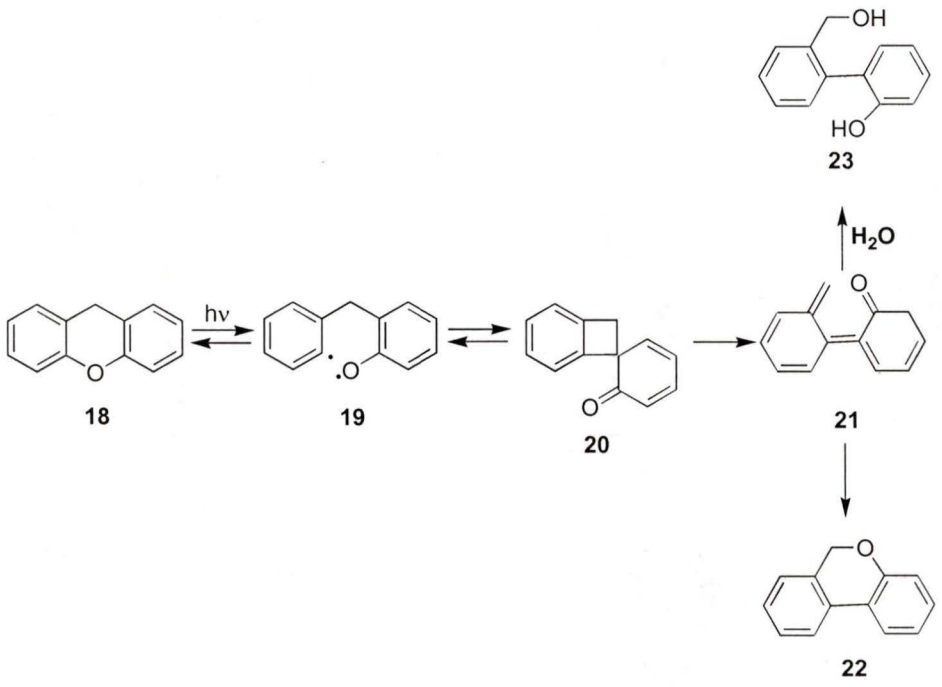

Scheme 1.2

1.1.4 Quinone Reactivity

The redox chemistry of quinones is prevalent throughout everyday life. It serves as the basis for the development of photographic films and is also used in Nature for enzyme-catalyzed reactions by electron transfer. The classic example involves the oxidation of hydroquinone (**24**) to *p*-benzoquinone (**25**) (Eq. 1.7). The oxidation can

occur thorough the use of a mild oxidizing agent leading to the loss of two electrons and two protons from hydroquinone (**24**). This is a reversible reaction since it can be easily reduced back to **24**. The oxidizing properties of quinones can be adjusted by the addition of substituents. Quinones bearing alkyl or other electron-donating substituents tend to decrease the oxidation potential while the opposite effect is observed when electron withdrawing substituents are present on the ring. Because of their relatively high oxidation potentials, *p*-benzoquinones such as 1,4-benzoquinone, chloranil and

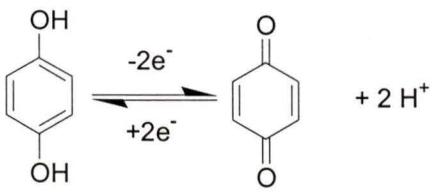

24 **25** (1.7)

DDQ (2,3-dichloro-5,6-dicyanoquinone) have been used widely as oxidants or dehydrogenating agents in synthetic organic chemistry. Several kinetic studies have been carried out on the dehydrogenation of hydroaromatic compounds[15], triphenylmethanes[16] and allyl alcohols[17] by quinones. The mechanism of quinone reduction was first proposed by Braude, Jackman and Linstead[15] which involved rate-determining hydride transfer from the hydrocarbon (AH_2) to the quinone (Q) (Eq. 1.8). Rapid proton transfer from the conjugate acid (AH^+) to the hydroquinone anion (QH^-) followed, leading to hydroquinone (QH_2) and the dehydrogenated product (A) (Eq. 1.8). This mechanism has been supported in an investigation on the oxidation of allylic alcohols with DDQ[17]. The isotope studies and conformational analysis suggest a slow hydride transfer followed by

rapid proton loss. Although the ionic mechanism has provided significant proof in the reduction of quinones, an electron transfer mechanism has not been ruled out. In fact studies have suggested dehydrogenation by quinones can occur when a quinone (Q) reacts with the substrate (AH_2) to give a radical anion ($Q^{\bullet -}$) and a radical cation ($A^{\bullet +}$) as a result of a one-electron transfer (Eq 1.10)[18,19]. In all of the above studies no carbon-

$$AH_2 + Q \xrightarrow{\text{slow}} AH^+ + QH^- \qquad (1.8)$$

$$AH^+ + QH^- \xrightarrow{\text{fast}} A + QH_2 \qquad (1.9)$$

$$A + Q \underset{}{\overset{\text{fast}}{\rightleftharpoons}} \underbrace{[\ A{:}Q\ ]}_{\text{charge-transfer complex}} \overset{\text{fast}}{\rightleftharpoons} A^{\bullet +} + Q^{\bullet -} \qquad (1.10)$$

carbon coupled dimerization products were observed. This observation supported an ionic mechanism since a radical mechanism should result in the formation of substrate dimer. It has been shown that coupled products may indeed be formed upon quinone dehydrogenation if carbon-carbon double bond formation is structurally impossible. These observations have suggested a possible homolytic mechanism as opposed to the earlier proposed ionic mechanism. One particular study reported the reaction of 3,3',5,5'-

tetramethyl-4,4'biphenylquinone with diphenylmethane resulting in the reduced quinone and tetraphenylethane **26** (Eq. 1.11).[20] The observation of the carbon-carbon coupled dimerization product strongly supported a homolytic mechanism in this case (for quinone dehydrogenation). Becker et al.[21] have also reported dimerized products in the quinone dehydrogenation of enols and enolizable ketones. This observation was explained by a homolytic mechanism. While most of the dehydrogenation studies have focused on DDQ or some other substituted form of *p*-benzoquinone as dehydrogenating agents, there has been little work[20] done on the reactivity of biphenylquinones and in particular 2,2'-biphenylquinones. A major component of this Thesis is concerned with the reduction mechanism of several 2,2'-biphenylquinones.

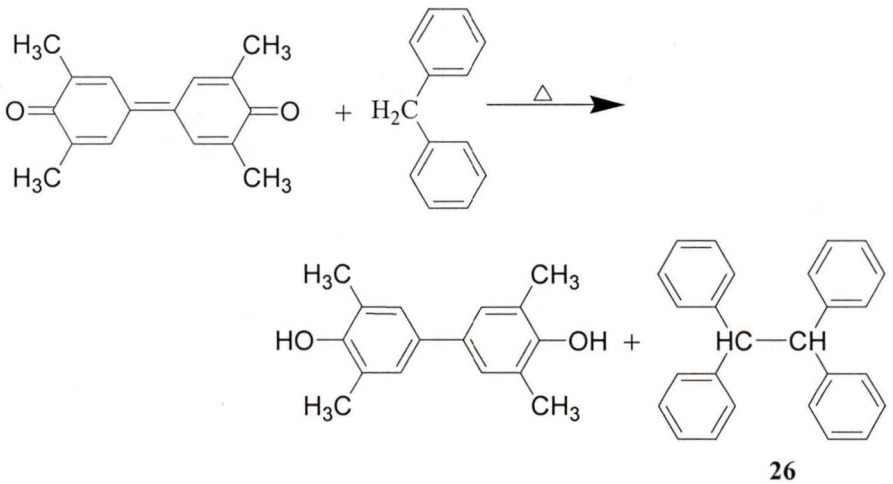

(1.11)

26

1.2 Dibenzo-*p*-dioxins

Dibenzo-*p*-dioxin is a diphenyl diether and is of photochemical interest due to its potential to undergo intramolecular rearrangement upon irradiation. It is the parent compound of the environmentally relevant 2,3,7,8-tetrachlorodibenzo-*p*-dioxin (**27**)

whose toxicity and bioaccumulation is of extreme interest. Studies have found that this man-made byproduct can be decomposed by light, thus its photochemistry has attracted considerable interest. The parent compound is the major topic of this thesis so a brief overview of the history of this notorious compound will follow.

1.2.1 Source, Formation and Degradation of Polychlorinated Dibenzo-*p*-dioxins

The 2,3,7,8-tetrachlorodibenzo-p-dioxin (**27**) has received enormous attention over the last number of years due to its high toxicity. It has an LD_{50} of 0.6-2.0 μg/kg in guinea pigs tested.[22] It has also gained a reputation through legendary contamination stories. In 1976, Seveso, Italy was the site of an explosion at a chemical plant releasing between 22 and 132 pounds of **27** into the atmosphere.[22] As a result many animals died and several humans were inflicted with a severe skin rash. This plant was engaged in the manufacture of 2,4,5-T (**28**) more commonly known as "Agent Orange". Industrial production of 2,4,5-T, at very high temperatures, leads to **27** as a by-product. (Scheme 1.3)

Polychlorinated dibenzo-*p*-dioxins have been found in a number of different locations: sawmills, wood-treatment plants, pulp and paper mills and health-related facilities to name a few. In addition it has been detected biologically in human tissue, soil, water, plants, fish and breast milk. Dioxin detoxication has become a major issue in scientific investigations and many efforts have been made to destroy and limit its formation. The most common method presently is thermal degradation.[22] In this case the

dioxin is incinerated at temperatures above 800°C. In addition to this method, chemical[23], biological[24] and electrochemical[25] degradation efforts have been made but no method has proven to be 100% efficient. Photochemical degradation has been attempted on the polychlorinated entities in UV light. The photochemistry of these compounds will be discussed in the following section.

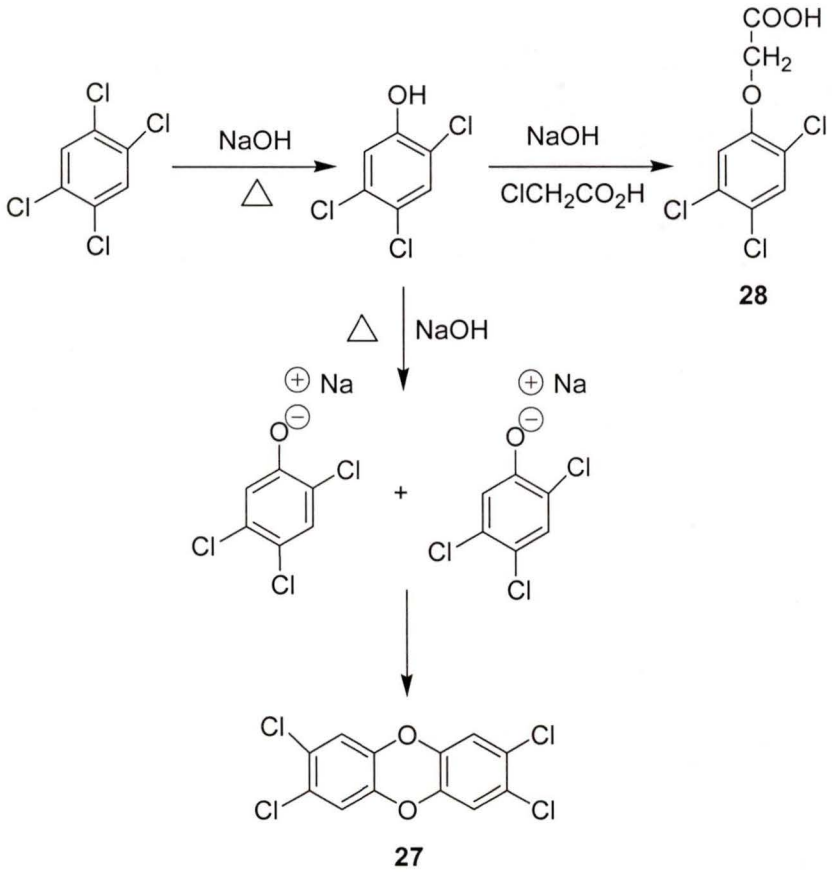

Scheme 1.3

1.2.2 Photochemistry of Polychlorinated Dibenzo-*p*-dioxins

While thermal degradation is the most common method for treatment of dioxin contaminated wastes, it is not completely efficient. Because of its high thermodynamic stability, extreme temperatures are required to burn dioxins effectively. Not only has this method proven to be costly, the high temperatures can result in the formation of more dioxin from precursors that may be already present. For this reason other methods for dioxin detoxication have been investigated. Of these studies, photochemical degradation has shown the most promise. One such case was exhibited in Verona, Missouri whereby the removal of about 7 kg of dioxin was done with the use of UV light in organic solvent over a period of several weeks.[22] The dioxin was destroyed with 99.44% efficiency and helped remove a serious hazard from this community.

Several reports on the photochemistry of polychlorinated dioxins have arisen in the last number of years. Crosby et al.[26] launched a preliminary report that the photolysis of **27** yielded dechlorinated products. In addition to this he also discovered the necessity of a hydrogen donating solvent to carry out the dechlorination process. Other studies[26-27] have followed this report and the dechlorination of polychlorinated dioxins has become of significant interest due to their immediate relevance to the degradation of these environmental pollutants.

One of the more notable findings in this area some years ago was the formation of tetra and penta-chlorinated dioxins from the photolysis of a hexa-chlorinated dioxin (Scheme 1.4).[28] More important to this finding was the observation that dechlorination primarily occurred at the lateral 2,3,7,8-positions of the dioxin compound. Dobbs and

Grant[27] found from the published half-lives of several polychlorinated dioxins that those with lateral chlorine atoms would degrade faster than those with chlorines in the 1,4,5,9 peri-positions.

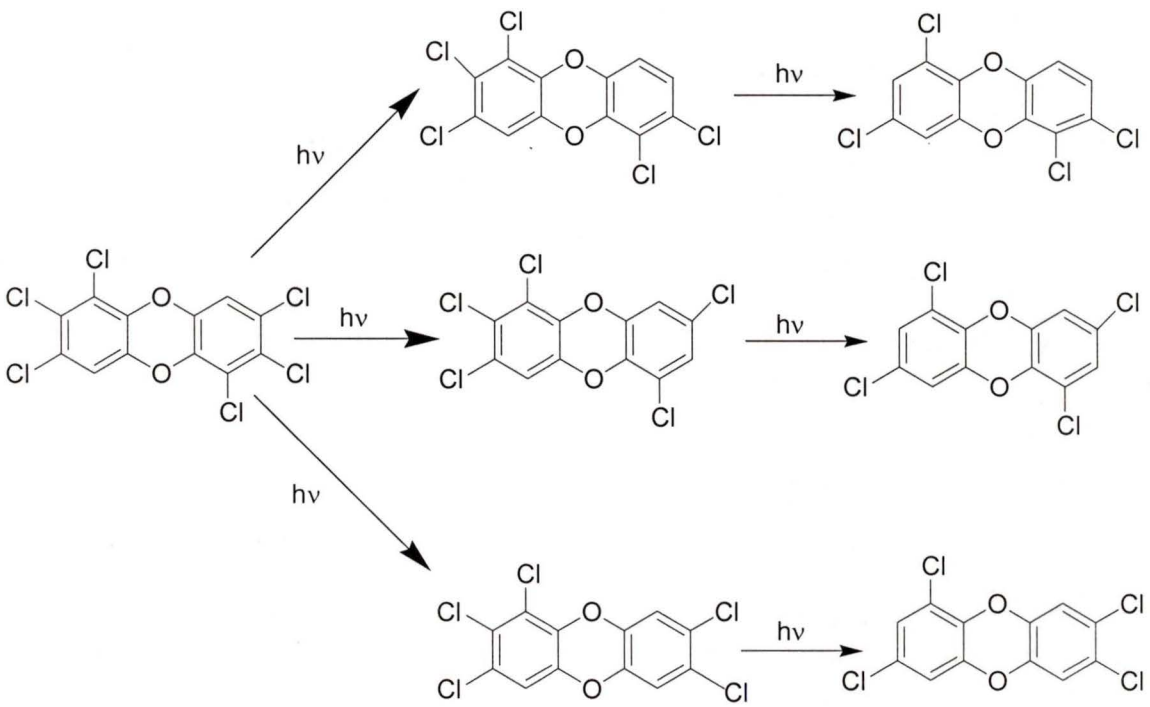

Scheme 1.4

A mechanism for dechlorination of polychlorinated dioxins has been proposed and involves two possible photochemical pathways (Scheme 1.5).[29] One such pathway involves homolytic C-Cl bond cleavage yielding the aryl radical **29**. This radical could then abstract hydrogen from solvent to yield the dechlorinated product **32** and subsequent

dechlorination would follow. Another possible route involves heterolytic C-Cl bond cleavage resulting in the proposed cation/carbene resonance structures **30** and **31.** Electron transfer from the chlorine to the cation/carbene intermediate would give the aryl radical which would reduce to the final product. This proposed mechanism helps to explain the primary dechlorination of the lateral chlorine atoms. The carbene intermediate that is formed from the loss of a lateral chlorine atom is more stable than the peri-dechlorinated species. In addition to this, slower rates of dechlorination are expected from the peri removal due to the electrostatic interaction that is generated from the positively charged oxygen and the negatively charged C-Cl group. The presence of hydride upon irradiation has been shown to greatly enhance the photoreaction.[30] This observation supports the proposed mechanism since the hydride is expected to reduce the carbene/cation intermediate to yield the dechlorinated product.

In 1989 Choudry et al.[31] reported the quantum yields of transformation of four polychlorinated dioxins (Table 1.1). The results revealed interesting facts based on the dechlorination of polychlorinated dibenzo-*p*-dioxins. According to their results, 1,3,6,8,-tetrachlorodibenzo-*p*-dioxin had a greater quantum yield than its 1,2,3,7 isomer. This finding challenges the trend observed that dioxins with lateral chlorine atoms decompose faster than ones with peri-chlorine atoms. These findings reveal that more is to be learned of the dechlorination pathway.

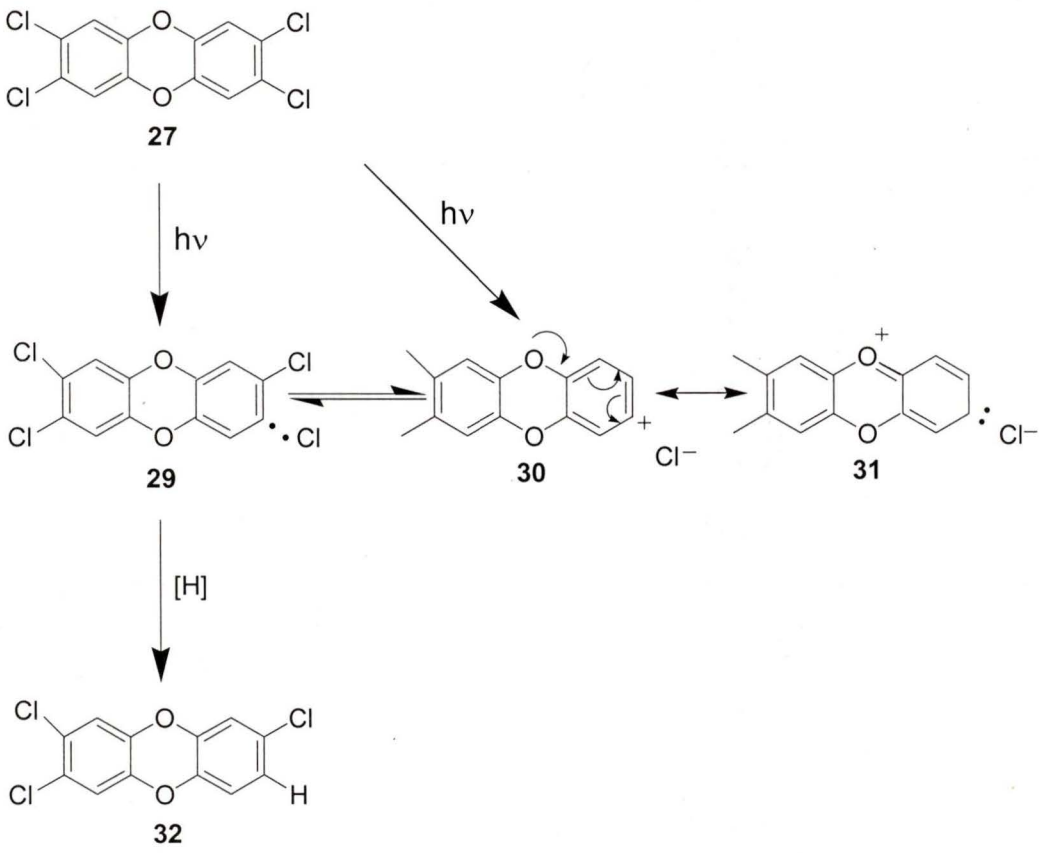

Scheme 1.5

Aside from dechlorination, another photochemical pathway for polychlorinated dioxins has been suggested. Several studies have suggested fission of the ether bond in the dioxin ring as part of the photochemical degradation pathway.[11,32,33] Kieatiwong et al.[34] observed a mixture of dechlorinated product along with 4,4',5,5'-tetrachloro-2,2'-biphenyl phenol when polychlorinated dibenzo-*p*-dioxin was photolyzed in isooctane. The observation of this product suggests C-O bond cleavage within the dioxin ring system. Bunce et al.[33] have shown that photolysis can be used as an efficient, safe and

inexpensive method for on site treatment of dioxin wastes. Within their study they revealed C-O bond cleavage as the principal photolytic pathway giving chlorinated hydroxy-biphenyls. Recently, Rayne et al.[35] reported the photochemical conversion of 2,3,7,8-polychlorinated dibenzo-*p*-dioxin to 2,2'-dihydroxy-4,4'-5,5'-tetrachlorobiphenol at greater than 50% yield. In addition to these findings on chlorinated dioxins, C-O bond cleavage has been observed in the parent dioxin system.[36] The history and known photochemistry of this compound will be discussed in the next section.

Table 1.1 Quantum Yields for the Disappearance of Polychlorinated Dibenzo-*p*-dioxins in Aqueous CH_3CN

Substrate	Initial Conc. (10^{-6} M)	Quantum Yield (Φ)
1,2,3,7-Tetrachlorodibenzo-*p*-dioxin	6.40	$(5.42 \pm 0.42) \times 10^{-4}$
1,3,6,8-Tetrachlorodibenzo-*p*-dioxin	10.55	$(2.17 \pm 0.14) \times 10^{-3}$
1,2,3,4,6,7,8-Heptachlorodibenzo-*p*-dioxin	2.78	$(1.53 \pm 0.17) \times 10^{-5}$
1,2,3,4,5,6,7,8-Octachlorodibenzo-*p*-dioxin	0.31	$(2.26 \pm 0.33) \times 10^{-5}$

1.2.3 Photochemistry of Dibenzo-*p*-dioxin (33)

The photochemical fate of dibenzo-*p*-dioxin (**33**) is of interest because it is the parent compound of the environmentally well-known PCDD's discussed in the preceding sections. Interestingly, only a few reports have investigated this pathway.[36, 37] These reports suggested aryl-oxygen bond homolysis as the primary photochemical step yielding the biradical **34** (Scheme 1.6). Hydrogen abstraction from the solvent would

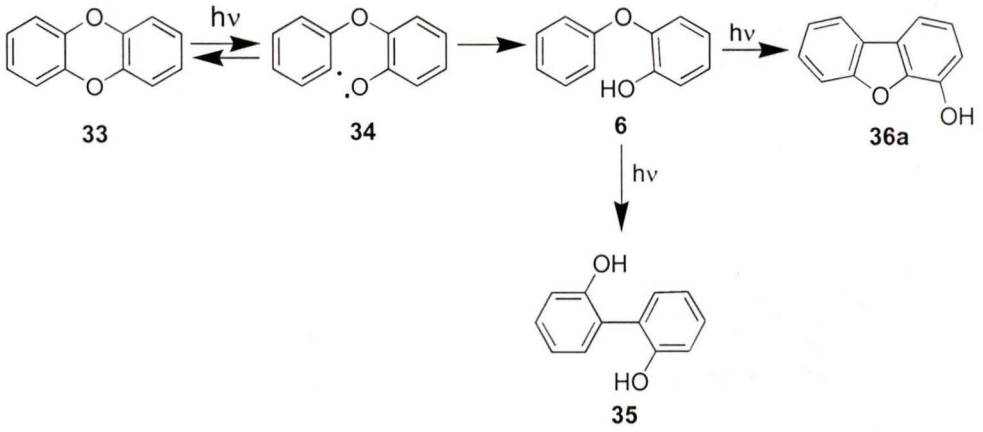

Scheme 1.6

afford 2-phenoxyphenol (**6**) which upon secondary photolysis could be converted to 2,2'-biphenol (**35**) as the major product along with a minor amount of 1-hydroxydibenzofuran (**36a**). This mechanism was not supported by later findings that irradiation of 2-phenoxyphenol does not produce any biphenol in the product mixture.[8,11] These findings indicate that the proposed mechanism for the photochemistry of dibenzo-*p*-dioxin was inaccurate. Due to this discrepancy, Guan and Wan[11] proposed an alternative photochemical pathway based on the mechanism of the photoisomerization of xanthene (**18**). The study reported 2,2'-biphenol (**35**) as the major product in 20-40% yields. In addition the yield was enhanced in the presence of $NaBH_4$. A newly devised mechanism for this reaction has been proposed and it involves initial aryl-oxygen bond homolysis to yield the biradical **34** (Scheme 1.7). This biradical can then abstract hydrogen from the solvent to give **6** but this is a minor pathway. The major pathway involves intramolecular *ipso* attack of the biradical to afford spiroketone **37**. The

subsequent electrocyclic ring opening will yield the biphenylquinone **38** which can either be reduced by solvent to give the 2,2'-biphenol (**35**) as the major product or undergo ring closure via secondary photolysis to give 4-hydroxy-dibenzofuran (**36b**). The latter product is a minor pathway seen only in non-hydroxylic solvents. The key finding in this report was the observation of the biphenylquinone intermediate **38** by UV-Vis spectroscopy.

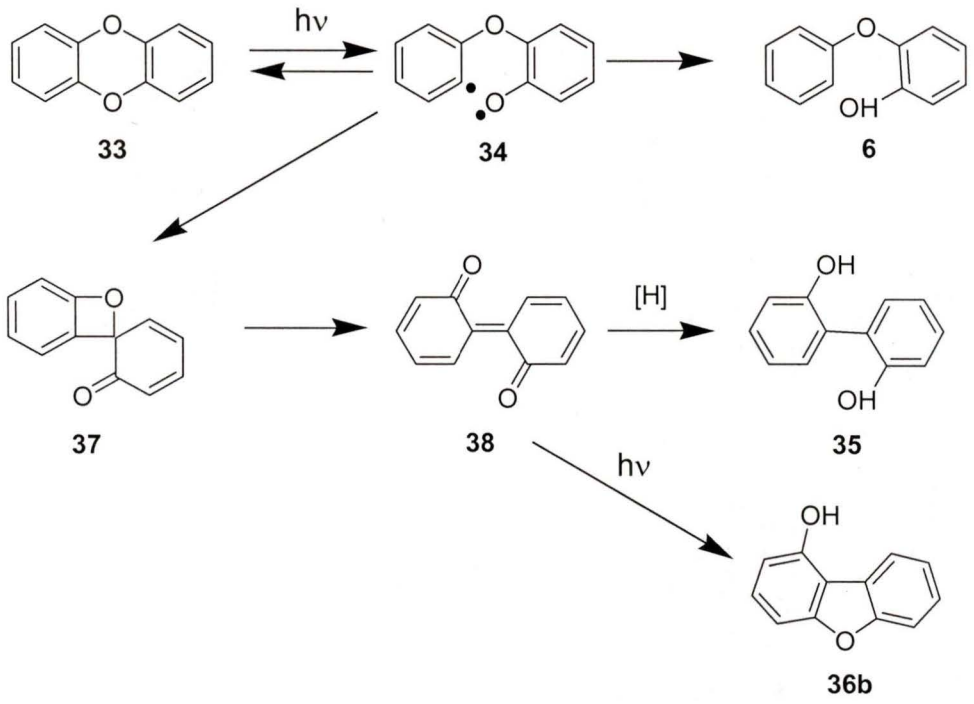

Scheme 1.7

1.3 Research Proposal

Previous work[11] has shown some evidence for a newly proposed mechanism for the photodegradation of dibenzo-*p*-dioxins. This Thesis will pursue a more detailed analysis of the proposed mechanism for the photoisomerization and reduction of **33** along with three of its derivatives; 2,3,7,8-tetramethyldibenzo-*p*-dioxin (**39**),

2,7-dimethoxydibenzo-*p*-dioxin (**40**) and 2,7-difluorodibenzo-*p*-dioxin (**41**).

Prior studies[11] have shown the presence of an observable biphenylquinone intermediate by UV-Vis spectroscopy. The kinetics of its formation and disappearance, however, have not been investigated. Laser Flash Photolysis (LFP) and additional UV-visible spectroscopic experiments are used in an attempt to identify the reactive intermediates formed upon irradiation and to measure their respective lifetimes. To serve as a comparison, compounds **39**, **40** and **41** were synthesized. It is anticipated that these compounds will react in a similar fashion to the dioxins previously studied, but show kinetic differences based on substituent effects. In addition, product studies are carried out to test the generality of the photoreaction while pH studies are done to explore the reaction behaviour under acidic conditions.

Chapter 2

Results and Discussion

2.1 Synthesis

Several compounds were synthesized for use in this Thesis. These compounds were prepared based on the Cu-catalysed condensation of chlorinated phenols[38]. Samples of dibenzo-*p*-dioxin were already synthesized by the above method and checked for purity by ^{1}H NMR, melting point and mass spectroscopy.

2.1.1 2,3,7,8-Tetramethyldibenzo-*p*-dioxin (39)

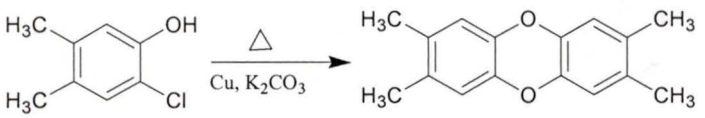

39 (2.1)

Compound **39** was synthesized according to the method outlined in Eq. 2.1. Starting material was purchased from Aldrich and checked for purity. Condensation of 2-chloro-4,5-dimethylphenol in the presence of copper and K_2CO_3 gave crude **39** which was purified through recrystallization in methanol in 5% yield. . The melting point agreed with the literature value[39] as did the ^{1}H NMR[11]. A mass spectrum confirmed the molecular weight of the compound (*m/e* = 240).

2.1.2 2,7-Dimethoxydibenzo-*p*-dioxin (40)

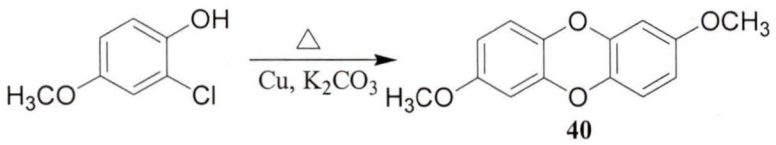

40 (2.2)

Dioxin **40** was synthesized according to the above method. Starting material was purchased from Aldrich and was checked for purity. Condensation of 2-chloro-4-methoxyphenol gave crude **40** which was purified by recrystallization in ethanol (1.3% yield). The purity was determined by ^{1}H and ^{13}C NMR, melting point and MS. Both the ^{1}H and ^{13}C NMR were consistent with the structure and the mass spectrum confirmed the molecular weight of the compound (*m/e* = 252).

2.1.3 2,7-Difluorodibenzo-*p*-dioxin (41)

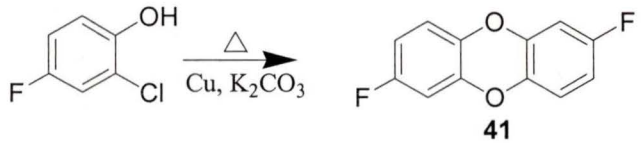

41 (2.3)

Dioxin **41** was synthesized using the method described above. 2-Chloro-4-fluorophenol was heated with copper catalyst and K_2CO_3. Crude **41** was obtained by recrystallization in methanol/water followed by sublimation (66% yield). The melting point and ^{1}H NMR were consistent with the literature[40] and the MS confirmed the molecular weight of the compound (*m/e* = 220). A ^{13}C spectrum was also obtained and was consistent with the structure of the compound.

2.2 Product Studies

The photoproducts of **33** and **39** were determined previously.[11] The results revealed 2,2'-biphenol (**35**) and 4,4',5,5'-tetramethyl-2,2'-biphenol, respectively as the major photoproducts in both hydroxylic and non-hydroxylic solvents. Trace yields of 2-phenoxyphenol (**6**) were found in the photolysis of **33**.

The formation of the 2,2'-biphenols from the photolysis of **33** and **39**, respectively, suggested some kind of isomerization of the initial ring system. A photochemical pathway was proposed based on the products formed. The working mechanism involves initial aryl-oxygen bond homolysis yielding biradical **34**. Intramolecular ipso attack gives the spiroketone **37** in which the ring then opens to yield the 2,2'-biphenylquinone **38**. Reduction of **38** by solvent gave the 2,2'-biphenol **35** as the major product. All studies suggested the same mechanism for **39**.[11]

The photoproducts of **33** in acidic media and of **40** and **41** are determined in this section and will be discussed in relation to the presently proposed mechanism.

2.2.1 Irradiation of Dibenzo-*p*-dioxin (33) in Aqueous CH_3CN

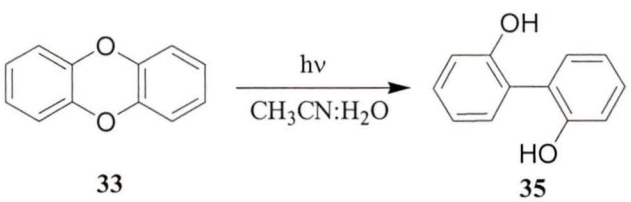

33 **35** (2.4)

Irradiation of an argon purged 1:1 H_2O-CH_3CN solution of **33** (4×10^{-3} M) in a RPR 100 photochemical reactor (300 nm) for 40 minutes at various pH (1-12) gave **35** as

the only major product. The product yields measured by ^{1}H NMR were unaffected by changes in pH and the observation of **35** as the only major photoproduct is consistent with the findings for **33** and **39** in aqueous and dry CH_3CN. These results suggest that the pH of the solution has no effect on the yield of the observed products. The observation of **35** as the only major photoproduct also supports the working mechanism proposed previously for **33** and **39**. Dark reactions were done for all solutions studied to ensure no reaction occurred without the presence of light.

2.2.3 Irradiation of 2,7-Dimethoxydibenzo-*p*-dioxin (40)

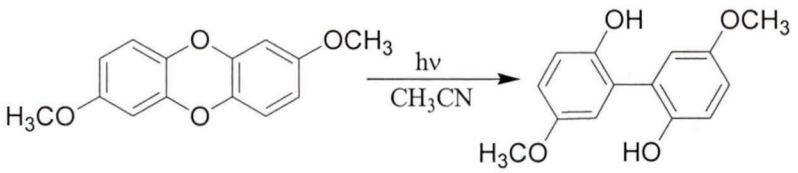

40 **42** (2.5)

To further investigate the generality of dioxin photoproducts, the photochemistry of 2,7-dimethoxydibenzo-*p*-dioxin (**40**) was studied. Irradiation of an argon purged CH_3CN solution of **40** (4×10^{-4} M) in a Rayonet RPR photochemical reactor (300nm lamps) at 18°C for 20 minutes resulted in one major product which was isolated by preparative TLC (silica gel, 50:50 hexane/ether). The ^{1}H NMR spectrum was consistent with **42** as the major photoproduct. The observation of this product is consistent with the product studies found upon photolysis of **33** and **39**. This finding suggests that **40** may undergo a similar photochemical mechanism to that proposed for the other two compounds.

2.2.3 Irradiation of 2,7-Difluorodibenzo-*p*-dioxin (41)

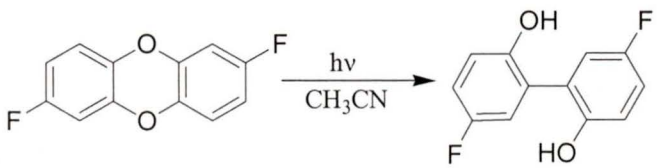

41 43 (2.6)

Irradiation of an argon purged CH_3CN solution of **41** (4×10^{-3}M) in a Rayonet RPR photochemical reactor (300nm lamps) at 18°C for 20 minutes resulted in one major product which was isolated by preparative TLC (silica gel, 70:30 hexane/ether). The ^1H NMR spectrum was consistent with the structure **43** as the major photoproduct. The observation of this product is also consistent with the product studies found upon photolysis of **33**, **39** and **40**. This finding also suggests that **41** may undergo a similar photochemical mechanism to that proposed for the other three compounds.

2.2.4 Regioselectivity of Bond Homolysis

The structures of **40** and **41** have two possible sites of homolytic C-O bond cleavage. Because these are dioxins in their disubstituted form, there are two possible photoproducts based on the site of bond homolysis. Scheme 2.1 shows the two possible paths of bond fission and their corresponding products. In order to delineate the preferential pathway of homolytic cleavage, products studies were performed on **40** and **41**. As described earlier, **43** was identified as the major photoproduct in the photolysis of **41**. This assignment comes from the observed ^1H and ^{13}C NMR spectra which were all consistent with the structure of **43** as opposed to **50**. This finding suggests that path a is

the preferential mode of cleavage in the initial step of this photoreaction. Its tendency to cleave via path a suggests that the aryloxy-phenyl cleavage prefers to occur when the fluorine is situated para to the phenoxyl radical as opposed to the meta position. This observation makes considerable sense when the transition states of path a and path b are

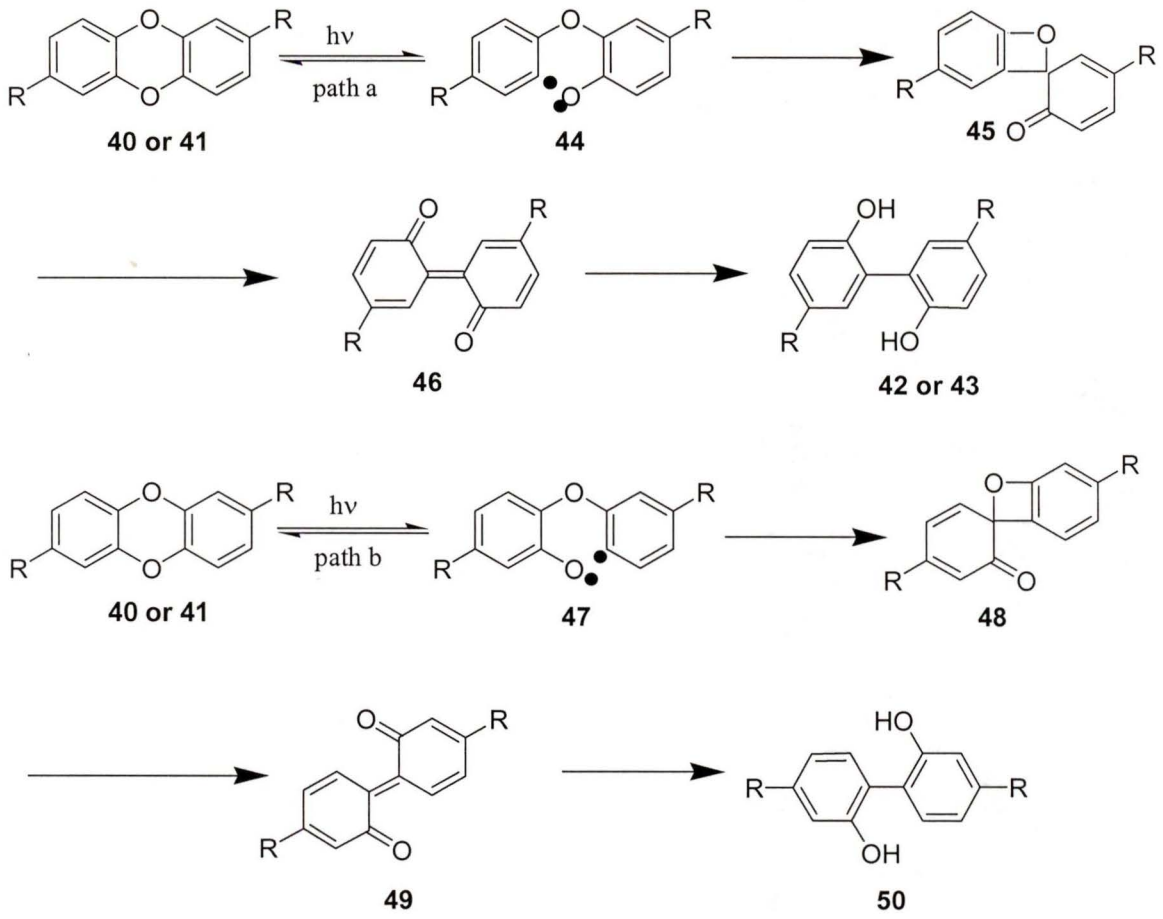

Scheme 2.1

compared along with the electronic properties of the fluorine substituents (R) (Scheme 2.2). The transition state of homolytic bond cleavage will generate a partial positive charge on the oxygen and a partial negative charge on the ring carbon. It is anticipated

that the electronic effects of the fluorine substituent (R) will participate in the stabilization or destabilisation of these partial charges. According to proposed path a, the partial positive charge on the oxygen in transition state **41a** will be slightly destabilized by the minimal electron withdrawing effects of fluorine (R) in the para position (σ_p = 0.06). Alternatively, the partial negative charge on the ring carbon of **41a** will be stabilized by the stronger electron withdrawing effects of fluorine (R) in the meta position (σ_m = 0.34). According to proposed path b, the partial positive charge on the oxygen in transition state **41b** will be heavily destabilized due to the strong electron withdrawing effects of the meta fluorine (R) (σ_m = 0.34). The partial negative charge on the ring carbon will be stabilized slightly by the electron withdrawing properties of para fluorine (R) (σ_p = 0.07) but this effect is expected to be minimal.

As mentioned earlier **42** was isolated as the only major photoproduct from photolysis of **40**. The observation of this product suggests C-O bond homolysis via path a as well. This finding can also be explained by once again looking at the transition state of the C-O cleavage. The transition state (**41a**) of homolytic bond cleavage generates a partial positive charge on the oxygen and a partial negative charge on the ring carbon. Cleavage via path a will allow stabilization of the partial positive charge on the oxygen due to the strong electron donating properties of a methoxy substituent (R) in the para position (σ_p = -0.27). The partial negative charge on the ring carbon in the transition state is also partly stabilized due to the electron withdrawing properties of methoxy (R) in the meta position (σ_m = 0.12). Although cleavage via path b results in a similar transition

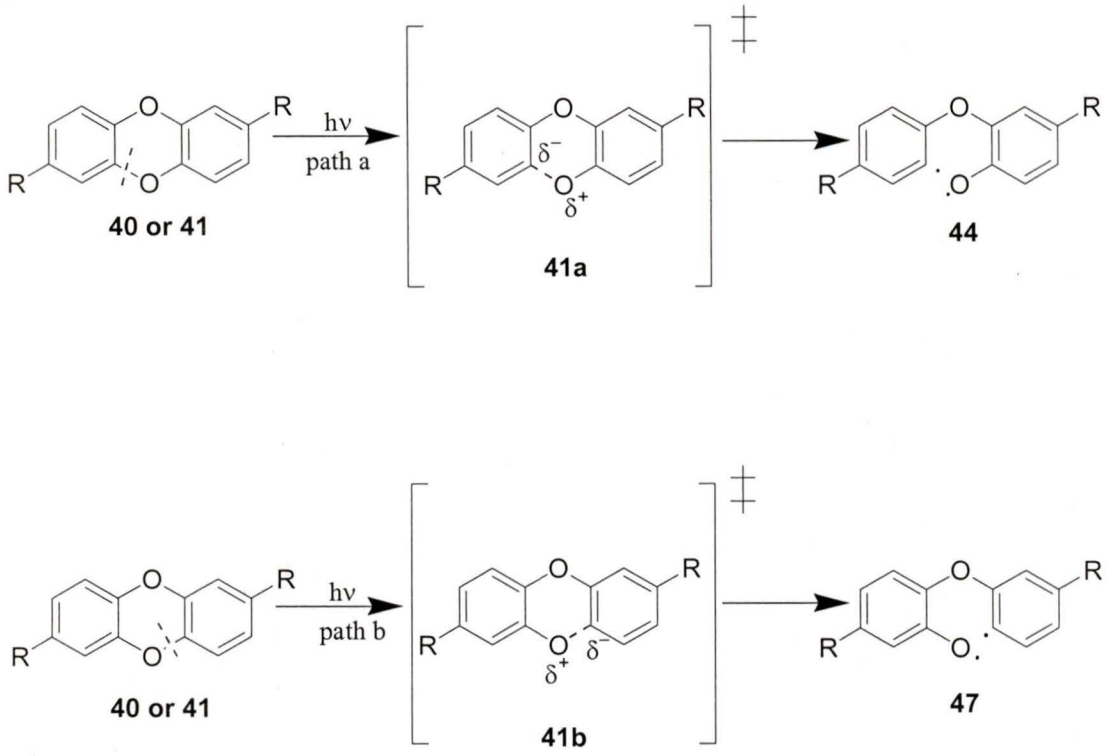

Scheme 2.2

state (**41b**), the stability of **41b** is markedly different than that observed in **41a**. The partial positive charge generated on the oxygen in **41b** is destabilized by the electron withdrawing effect of methoxy (R) in the meta position ($\sigma_m = 0.12$). The negative charge on the ring carbon is also destabilized by the electron donating properties of a methoxy substituent (R) in the para postion ($\sigma_p = -0.27$). Based on these arguments there is no doubt that transition state **41a** would be more favourable than that of **41b**. As a result it is reasonable to conclude that path a is the preferential mode of homolytic bond cleavage for both dioxins **40** and **41**. While there is a possibility of cleavage via both paths a and b, product studies did not reveal the presence of **50** in the photolyses of **40** and **41**. This observation is consistent with a study on the photochemical rearrangement of diphenyl

ethers where the preferred modes of cleavage generated *p*-fluorophenoxyl and *p*-methoxyphenoxyl radicals.[9] A similar mechanistic explanation to the one given above was used to explain this phenomenon.

2.3 UV-Vis Studies

Product studies have suggested 2,2'-biphenol and its derivatives to be the major photoproducts from the dioxins studied. The working mechanism for this reaction includes the formation of 2,2'-biphenylquinones as reactive intermediates. These types of quinones have historically been very elusive and their presence in the literature is limited to only a few reports.[11-14] Previous work has shown the generation of 2,2'-biphenylquinone (**38**) and 4,4',5,5'-tetramethyl-2,2'-biphenylquinone (**51**), from the photolyses of **33** and **39**, respectively.[11] Irradiation of **33** and **39** generated pink transients whose colour disappeared after several minutes. A UV-vis spectrum of these transients revealed two distinct absorption bands (λ_{max} in the 340-380 nm and 530-600 nm regions) which disappeared after several minutes (Figure 2.1 and 2.2). These transients were therefore assigned as reactive intermediates which served as precursors to the biphenol products. The intermediates were assigned as their respective 2,2'-biphenylquinones (**38** and **51**) based on the working mechanism proposed and their consistency with the UV spectrums of other known biphenylquinones all of which have two distinct absorption bands in the regions mentioned.[12-14]

The appearance of these biphenylquinone intermediates in the photolysis of **33** and its derivatives **39**, **40** and **41** will be further investigated in an attempt to generalize

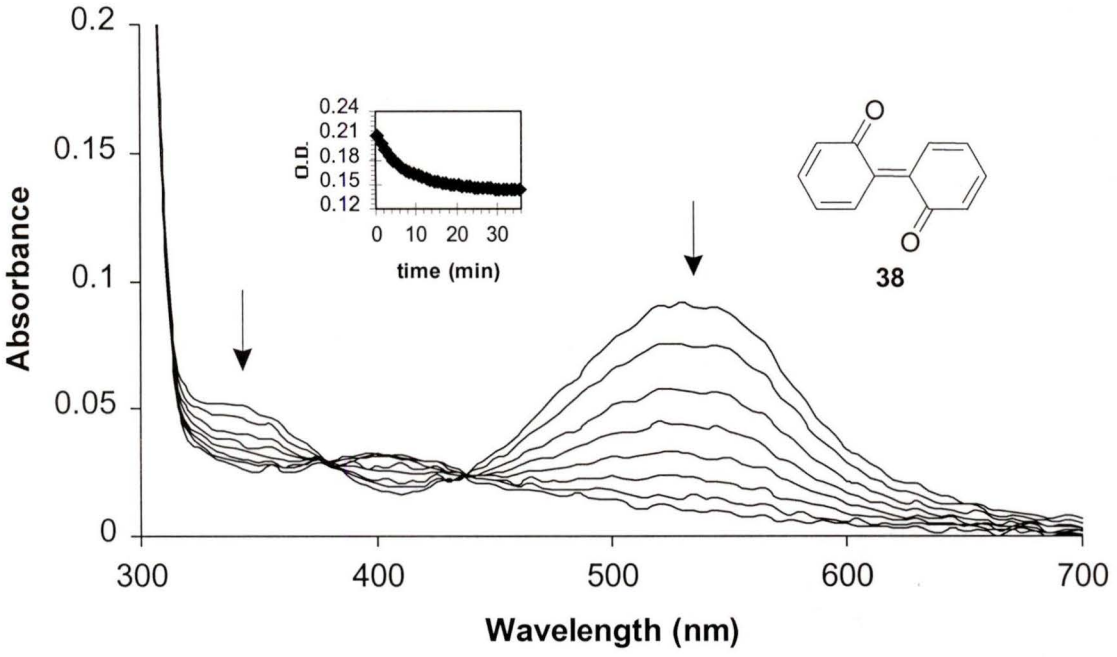

Figure 2.1 UV-Vis spectrum of the decay of 2,2'-biphenylquinone (**38**) in CH_3CN.

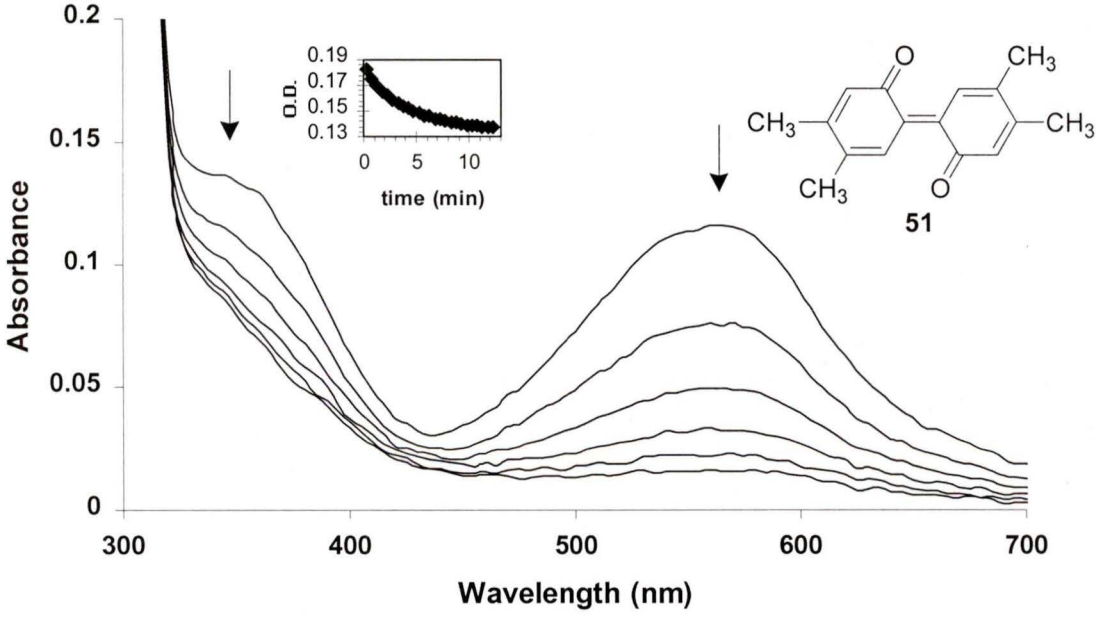

Figure 2.2 UV-Vis spectrum of the decay of 4,4',5,5'-tetramethyl-2,2'-biphenylquinone (**51**) in CH_3CN.

the photochemical mechanism of dioxins. In addition, the reactivity of the biphenylquinones and the possible effects the substituents and solvents may have on these systems will also be considered in order to resolve the kinetics of its decay. The assignment of **42** as the major photoproduct from the photolysis of **40** was determined earlier from product studies. The proposed mechanism suggests the existence of a biphenylquinone intermediate as a precursor to this final product. Earlier UV-Vis studies on **33** and **39** have provided evidence on the existence of this key intermediate.[11] Based on previous observations, an attempt to observe the biphenylquinone intermediate in the photoreaction of **40** was necessary.

An argon purged dry CH_3CN solution of **40** (3×10^{-5}) was irradiated in a quartz cuvette for 30 s at 300 nm. The solution turned a dark blue and a UV-Vis spectrum was taken immediately after photolysis. The spectrum showed a new absorption band at λ_{max}= 610 nm (Figure 2.3) which disappeared along with the colour of the transient after several minutes. The observation of this transient is consistent with the findings in the systems of **33** and **39**. Therefore, based on these earlier studies, the transient is assigned as 5,5'-dimethoxy-2,2'-biphenylquinone (**52**). The disappearance of this intermediate may be due to reduction by solvent to yield the proposed 5,5'-dimethoxy-2,2'-biphenol (**42**).

Irradiation of an argon purged dry CH_3CN solution of **41** (3×10^{-5} M) at 300 nm in a quartz cuvette for 30 s resulted in a pink coloured transient which lost its colour over time. A UV-Vis spectrum (Figure 2.4) of this transient taken immediately after photolysis revealed a distinct absorption band at λ_{max}= 520 nm which disappeared after several minutes. Similar to the above finding, this transient was assigned as 5,5'-difluoro-

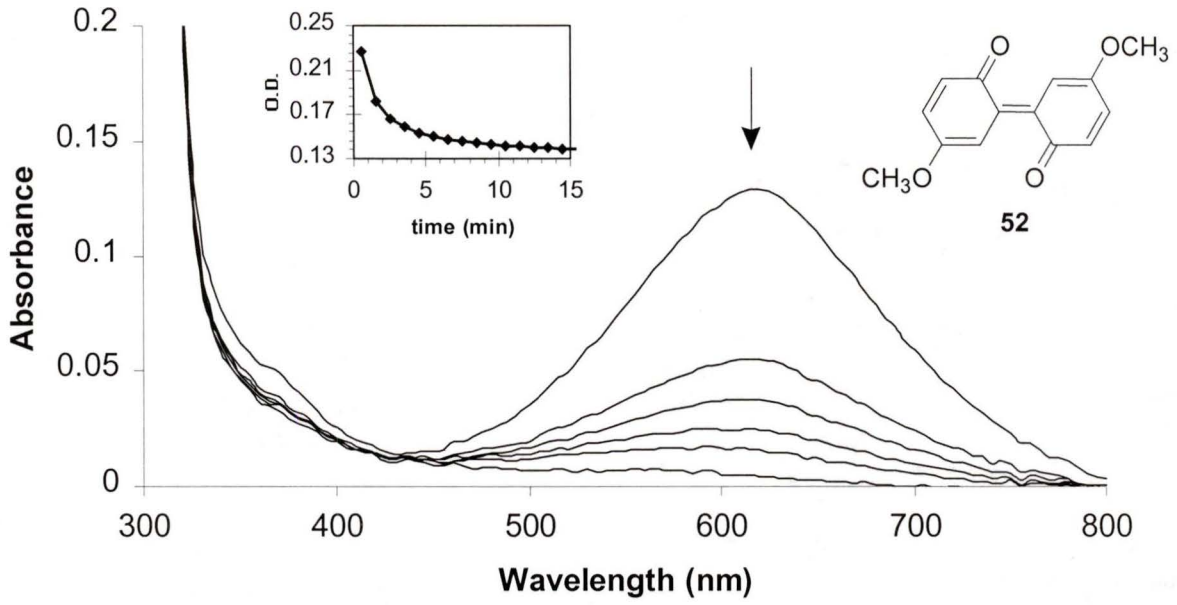

Figure 2.3 UV-Vis spectrum of 5,5'-dimethoxy-2,2'-biphenylquinone **(52)** in CH_3CN.

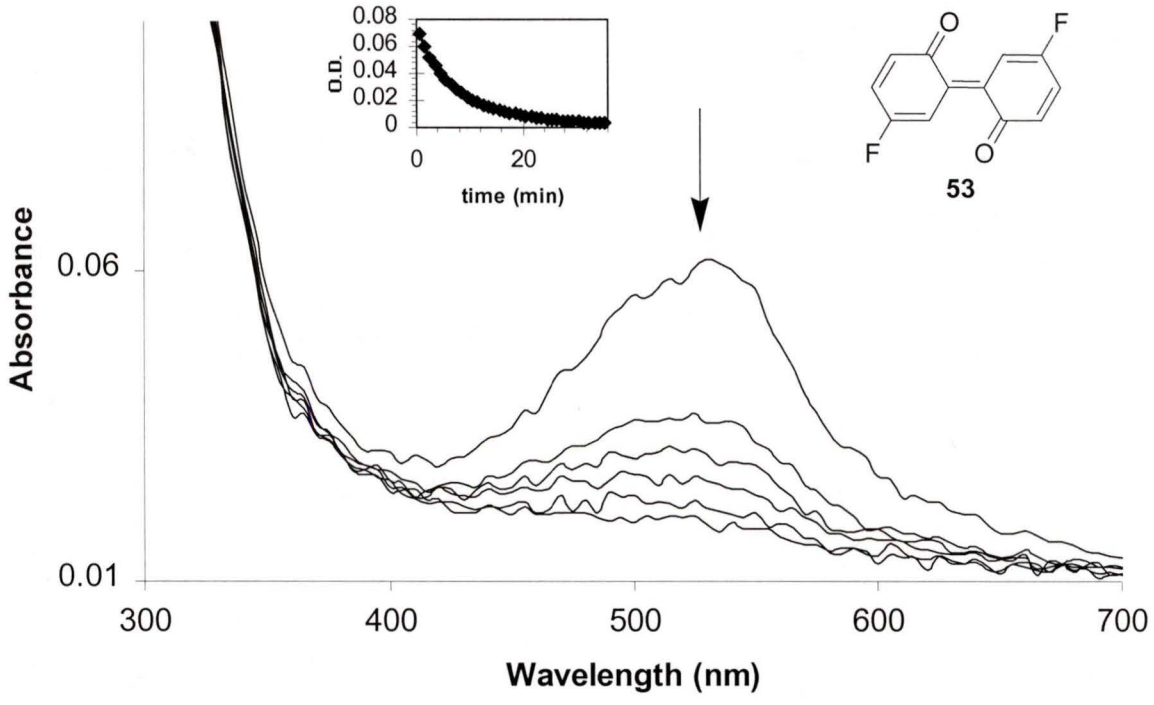

Figure 2.4 UV-Vis spectrum of 5,5'-difluoro-2,2'-biphenylquinone (**53**) in CH_3CN.

2,2'biphenylquinone (**53**) which may undergo reduction to give the biphenol product **43**. As mentioned earlier the assignments of **52** and **53** as biphenylquinones is further evidenced by the reported spectra of other biphenylquinones in the literature.[12-14]

The formation and observation of the biphenylquinones are followed by a loss in colour and disappearance of the transient's absorption bands over time. This observation suggests that the biphenylquinone intermediates are only formed for a short period of time and quickly react to yield another product. The biphenol compounds observed in the product studies have been suggested as the reasonable product that evolves from the reduction of the biphenylquinone intermediates. It is anticipated that the absorption of biphenol product would appear on the UV-vis spectrum during the decay of the observed biphenylquinone. As shown in Figure 2.5, photolysis of an argon purged dry CH_3CN solution of **33** (3×10^{-5} M) in a quartz cuvette (λ_{ex} = 254 nm, Rayonet photochemical reactor) resulted in the transformation to a product with λ_{max} = 278 nm. Exhaustive photolysis in CH_3CN gave a final trace at λ_{max}= 269 nm which is consistent with the formation of **35**, by comparison with its authentic spectrum. As a result this new band has been assigned as the 2,2'-biphenol product **35** since it is the major photoproduct observed in this reaction.

An identical UV-Vis study was carried out on the photolysis of **40.** Figure 2.6 shows the UV-Vis spectrum of **40** before and after photolysis. Exhaustive photolysis in CH_3CN gave a final trace at λ_{max}= 284 nm. This observation is consistent with the conversion of **40** to **42**. In Section 2.3.1 the observation and disappearance of the

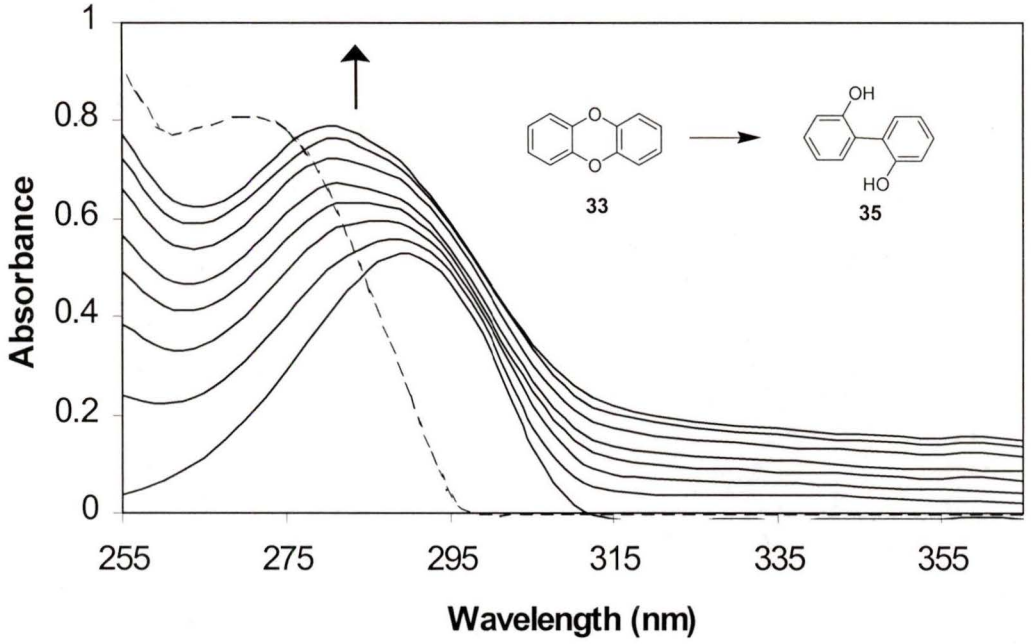

Figure 2.5 UV-Vis traces for the conversion of **33** to **35** on photolysis at 254 nm in CH_3CN. Dashed line is the spectrum of authentic **35** in CH_3CN. Each trace represents 30 seconds of irradiation time.

biphenylquinones were done in a dry CH_3CN solvent system. The explanation for the conversion of the biphenylquinones to the biphenols involves reduction of the quinone intermediates by solvent to give rise to the biphenols as the final products.

Quinone reduction has been shown to occur via three different mechanisms (Eq. 1.8-1.10). The first involves quinone (BQ) reduction by a hydride transfer reaction in the rate-determining step (Eq. 2.7). This hydride transfer is then followed by rapid proton transfer leading to the reduced quinone (BQH_2). Reduction of 2,2'-biphenylquinones (**38**, **51**, **52** and **53** by CH_3CN (RH_2) via this mechanism is not expected since the

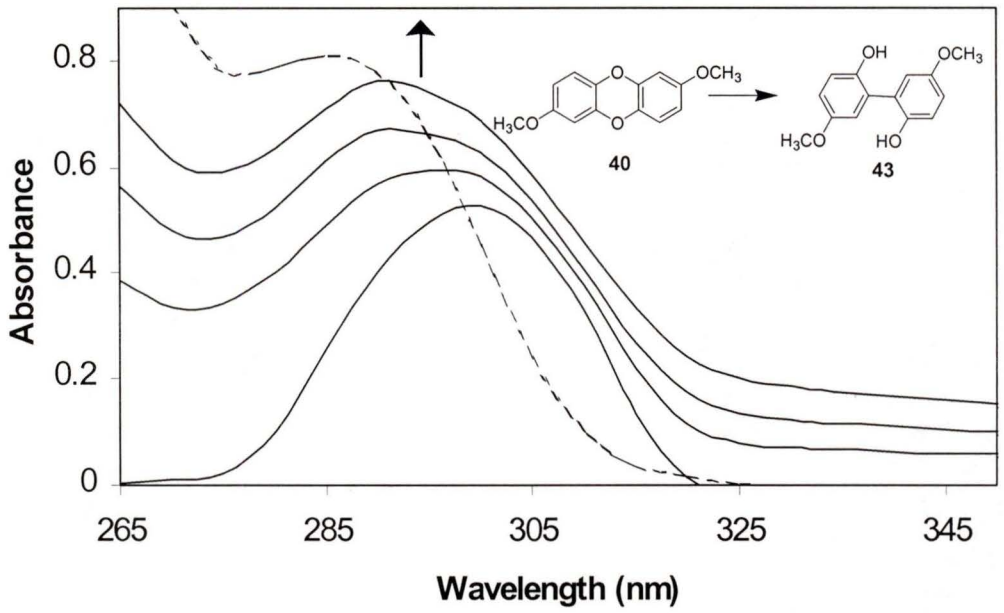

Figure 2.6 UV-Vis traces for the conversion of **40** to **43** on photolysis at 300 nm in CH_3CN. Each trace represents 30 seconds of irradiation time. Exhaustive photolysis gave a product **43** with λ_{max}= 282 nm (dashed trace).

transfer of a hydride from the CH_3CN would result in a positively charged carbon adjacent to an electron-withdrawing nitrile functional group (RH^+). The second possible mechanism involves electron transfer from the solvent (R) to the quinone intermediate (BQ) (Eq. 2.8). This process is also regarded as unfavourable since it would result in the generation of a radical cation ($R^{\cdot +}$) on the carbon adjacent to the nitrile group in acetonitrile. The last possible mechanism seems to be the most consistent with the observations thus far (Eq. 2.9). It involves hydrogen abstraction from two acetonitrile molecules (RH_2) by the biphenylquinone intermediate (BQ) resulting in the reduced

quinone (BQH_2) as the major product. This radical mechanism seems much more reasonable than the former suggestions since it results in the formation of two acetonitrile radicals which can combine to form a dimer (HR-RH). This mechanism for the reduction of the biphenylquinones by acetonitrile seems most likely and as a result will be considered the working mechanism throughout the rest of the discussions in this thesis.

$$RH_2 + BQ \xrightarrow{\text{slow}} \overset{\oplus}{RH} + \overset{\ominus}{BQH} \xrightarrow{\text{fast}} R + BQH_2 \qquad (2.7)$$

$$R + BQ \rightleftharpoons [R : BQ] \rightleftharpoons \overset{\bullet +}{R} + \overset{\bullet -}{BQ} \qquad (2.8)$$

charge-transfer complex

$$RH_2 + BQ \xrightarrow{\text{slow}} \dot{R}H + \dot{B}QH + RH_2 \xrightarrow{\text{fast}}$$

$$\dot{R}H + \dot{R}H + QH_2 \longrightarrow HR{-}RH + BQH_2 \qquad (2.9)$$

dimer

2.3.1 Substituent Effect on Biphenylquinone Reactivity

The UV-Vis absorptions for all the biphenylquinones were reported to disappear over a period of time. The lifetimes of decay were monitored at single wavelengths for each of the biphenylquinones studied. Table 2.2 shows the lifetimes for the reduction of

the biphenylquinones **38**, **51**, **52** and **53.** The biphenylquinone calculated lifetimes observed varied significantly from each other. This result was expected since the substituents on each of the compounds are markedly different with respect to their electronic properties. Table 2.1 shows that the lifetimes of the biphenylquinones are shorter for those bearing electron donating substituents (**51** and **52**). The lifetimes for the reduction of **38** and **53** are very similar. The mechanism for this reduction was justified earlier as hydrogen abstraction of the biphenylquinones from the solvent to yield the respective biphenol product.

Table 2.1 Biphenylquinone Lifetimes in Dry CH_3CN

Biphenylquinone	rate (min^{-1})[a]	lifetime (min)[a]
38	0.200 ± 0.01	5.2 ± 0.7
51	0.521 ± 0.04	2.0 ± 0.4
52	0.870 ± 0.05	1.2 ± 0.3
53	0.212 ± 0.02	4.9 ± 0.3

[a] Lifetimes determined from the average of three trials

The conversion from the biphenylquinone to the biphenol requires the abstraction of two hydrogens (presumably from two separate acetonitrile molecules). Because the rate of reduction is determined by the first hydrogen abstraction, it can be argued that biphenylquinones bearing electron-donating substituents would shorten the lifetime based

on the electronic nature of the system after this initial process. For example, in the reduction of **38**, abstraction of the first hydrogen will result in the even more electron-deficient **55** which would favour a second instantaneous hydrogen abstraction (Eq. 2.10). The efficiency of this reduction is based on the likelihood of formation and the stability of the formed radical species **55**. During the reduction of **52**, the radical species **57** will be more stable and thus more favourable since it bears electron donating substituents to help reduce the electron deficiency in the ring (Eq. 2.11). The observation that the lifetime of reduction is the shortest for **52** supports this analogy, since it bears $-OCH_3$ groups which are much better electron donating substituents ($\sigma_p = -0.27$) than $-CH_3$, -H and -F ($\sigma_p = -0.17$, 0.00 and 0.06 respectively). The Hammett plot shown in Figure 2.7

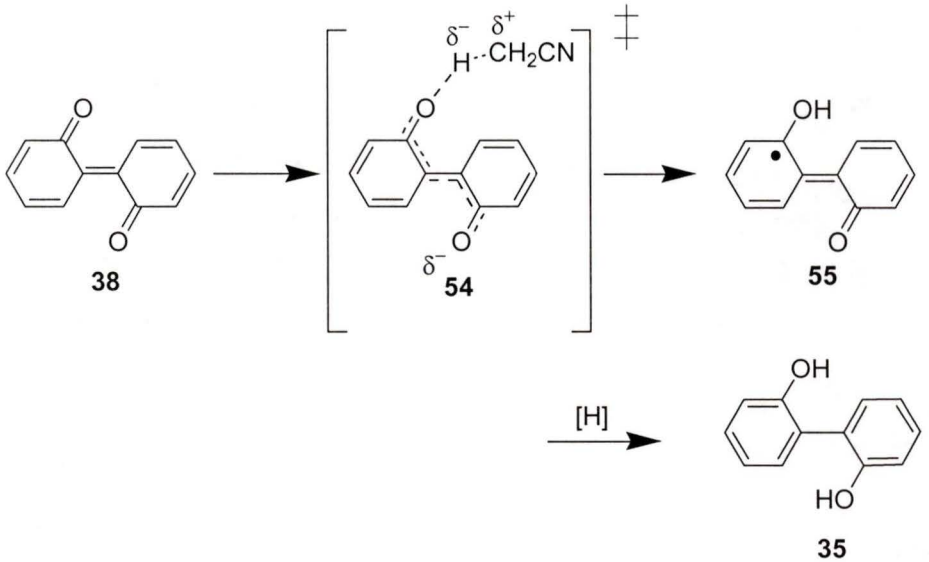

(2.10)

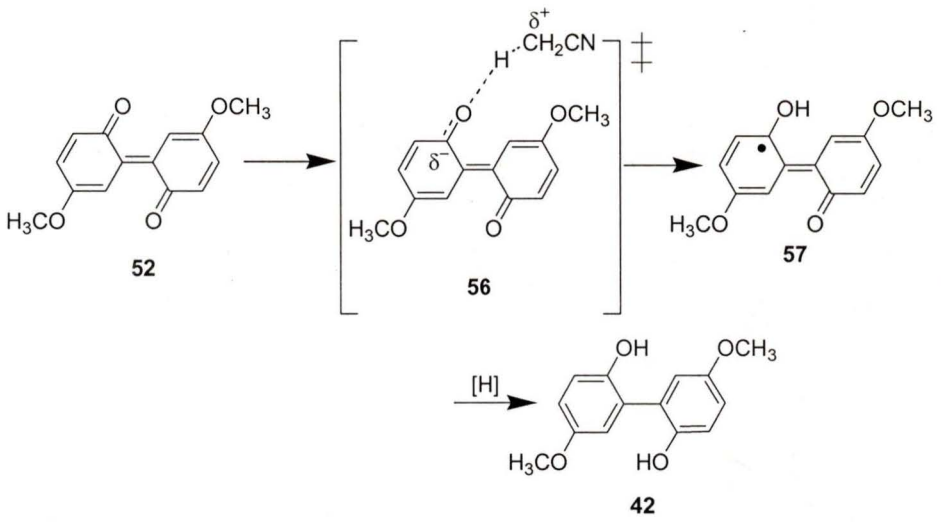

(2.11)

illustrates the effect the substituents have on biphenylquinone reduction. The negative slope means that reaction centre in the transition state is considerably more electron deficient than in the starting material and thus it is enhanced by electron donating substituents. The transition state (**54** or **56**) of the hydrogen abstraction shows the generation of a partial positive charge on the oxygen as it pulls a hydrogen from acetonitrile (Eq. 2.10 and 2.11). The nature of this transition state is consistent with the ρ value from the Hammet plot in that the reaction site is more electron deficient than the starting material. As expected, the lifetimes of **38** and **53** are longer than **51** due to greater electron donating effects of the methyl groups in **51**. The observation that **38** and **53** have virtually the same lifetimes is not very surprising when considering the σ_p values of fluorine and hydrogen. In the para position, the difference between the electronic contributions from a fluorine ($\sigma_p = 0.06$) and a hydrogen ($\sigma_p = 0.00$) is minimal. Because of this small difference, a significant change in lifetime between **25** and **45** is not expected. The ρ value in the Hammett plot also suggests that the presence of electron-

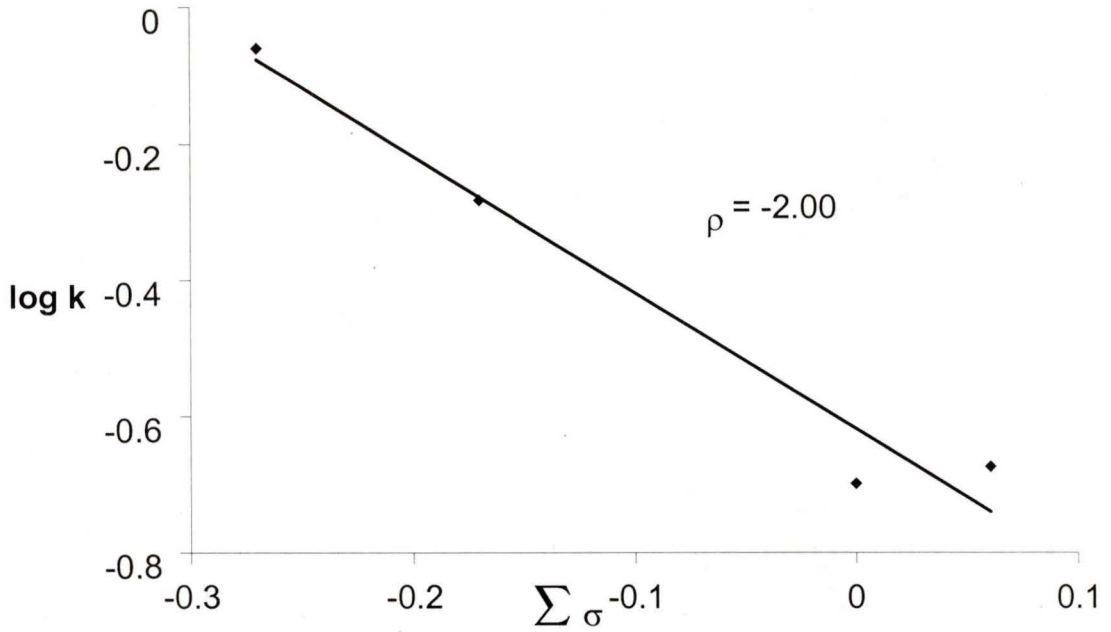

Figure 2.7 Hammet plot of log k (rates of biphenylquinone reduction) versus the sum of σ (Hammet Substituent constants) illustrating the substituent effects on biphenylquinone reduction.

withdrawing substituents would increase the lifetime of reduction of the biphenylquinones studied. The study of dioxins bearing such substituents (eg. Cl) would be useful, but due to the known high toxicity of these compounds this topic will not be addressed.

2.3.2 Solvent Effects on the Reduction of Biphenylquinone Intermediates

Because acetonitrile is considered the reducing solvent in this reaction it is expected that an increase in the reducing power of the solvent will result in a more efficient reduction reaction. To test this hypothesis, the lifetimes of the biphenylquinones were studied in both CH_3CN and 2-propanol, a better reducing solvent,

to see if reduction was more efficient in a stronger hydrogen donating medium. Identical argon purged 2-propanol and CH_3CN solutions of **33** (3×10^{-5} M) were irradiated in separate quartz cuvettes for 30 s at 300 nm. Both UV-Vis spectrums were taken immediately after photolysis and the distinct pink colour and absorption bands were observed in both studies. The decay for both solutions were monitored at 525 nm. The lifetimes revealed the expected results as shown in table 2.2. The 2,2'-biphenylquinone had a shorter lifetime in 2-propanol than in CH_3CN. This result supports the argument that quinone reduction occurs from the solvent. Similar results were found in the kinetic studies of the other three biphenylquinones as shown in table 2.2. All studies revealed a shorter lifetime of the biphenylquinone in 2-propanol as compared to CH_3CN.

The effect water may have on the lifetimes of the biphenylquinones was also investigated. An argon purged 1:1 CH_3CN-H_2O solution of **33** (3×10^{-5} M) was irradiated in a quartz cuvette for 30 s. A UV-Vis spectrum of the pink transient taken immediately after photolysis revealed the characteristic absorption bands which decayed over time. In order to determine the lifetime in the presence of water, the absorption band was monitored at 525 nm. The lifetimes calculated for the aqueous runs were directly compared with identical experiments in dry CH_3CN, as shown in Table 2.2. Based on the kinetic data, the results suggested that the decay of the biphenylquinone intermediate was significantly enhanced when water was present in the reaction mixture. Because the transient is still observed in the UV-Vis spectrum and the major photoproduct is formed in aqueous media, this result suggests a water-enhancing effect in the reduction reaction. Identical runs of the other three derivatives were also carried out and their lifetimes

Table 2.2 Biphenylquinone Lifetimes in Various Solvents

Biphenylquinone	CH_3CN[a] (min)	1:1 CH_3CN:H_2O[a] (min)	2-propanol[a] (min)
38	5.2 ± 0.7	0.5 ± 0.1	3.2 ± 0.2
51	2.0 ± 0.4	0.3 ± 0.2	1.5 ± 0.3
52	1.2 ± 0.3	0.2 ± 0.1	0.6 ± 0.2
53	4.9 ± 0.3	0.6 ± 0.1	3.1 ± 0.3

[a] Lifetimes determined from the average of three trials

as shown in Table 2.2, followed the same trend observed in the reduction of **38**. These results can be explained in part due to hydrogen-bonding effects. Biphenylquinone **38** contains two ketone oxygens which are susceptible to hydrogen bonding from solvent. It is anticipated that hydrogen bonding from a water molecule will inherently attach a minimal change in charged character on the ketone oxygen of **58** as shown in Scheme 2.3. Because of this small change in polarity the ketone oxygen that is participating in the hydrogen bonding will become more electronegative and thus will generate a larger affinity for the electrons in the rest of the quinone system. As can be seen from the structure of **38** in Scheme 2.3, the system is already electron-poor. The addition of this hydrogen bonding effect will result in an increase in the electron deficiency of the entire biphenylquinone system and would be expected to increase its affinity for a hydrogen radical from CH_3CN. This explanation can be further tested based on the idea that a more protic

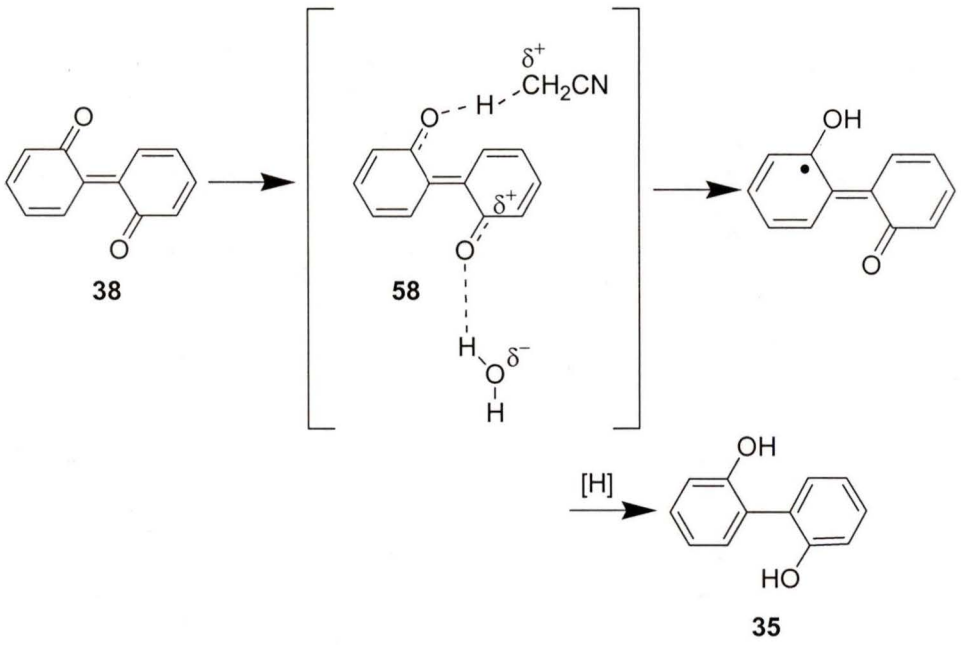

Scheme 2.3

solvent would enhance the reduction of the biphenylquinone intermediates to an even greater extent. Thus a study on the reactivity of biphenylquinones in acidic media was launched to determine whether the quinone reduction is in fact acid-catalysed.

The product study discussed in Section 2.2.1 revealed the 2,2'-biphenol (**35**) as the only major product from the photolysis of **33** under acidic conditions. An argon purged 1:1 CH_3CN-H_2O solution of **33** (3×10^{-5} M) was irradiated in a quartz cuvette for 30 s at 300 nm. Immediately following photolysis a drop of water (pH = 1) was added to the pink solution. The pink colour immediately disappeared and a UV-Vis spectrum of the solution showed no distinct absorption bands as seen in the typical biphenylquinone spectrum. Therefore based on these results it seems that there is an acid-catalysed reduction of the biphenylquinone **38** to the biphenol **35**. Additional experiments on **39**, **40**

and **41** under identical conditions yielded similar results suggesting a general acid-catalysed reduction of the biphenylquinone to the biphenol products. The lack of observation of the typical quinone absorption bands after the addition of acid suggests that the decay is too fast to be monitored by the present method. This observation further promotes the mechanism shown in Scheme 2.3 describing the water-assisted effect. Since the lifetime of the quinones are even shorter in acidic media (pH 1), as compared to aqueous media (pH 7), a similar mechanism to that in Scheme 2.3 can be shown to describe the acid-catalysed reduction. At pH 1, the solvent effects described earlier should be greater because protonation of the quinone (**38**) will occur more rapidly under these conditions (Scheme 2.4). As a result, the biphenylquinone system (**59**) should become even more electron-deficient, thus increasing its affinity for hydrogen from acetonitrile. This effect follows the same idea presented for the water-enhanced reduction but it demonstrates it to a much greater degree.

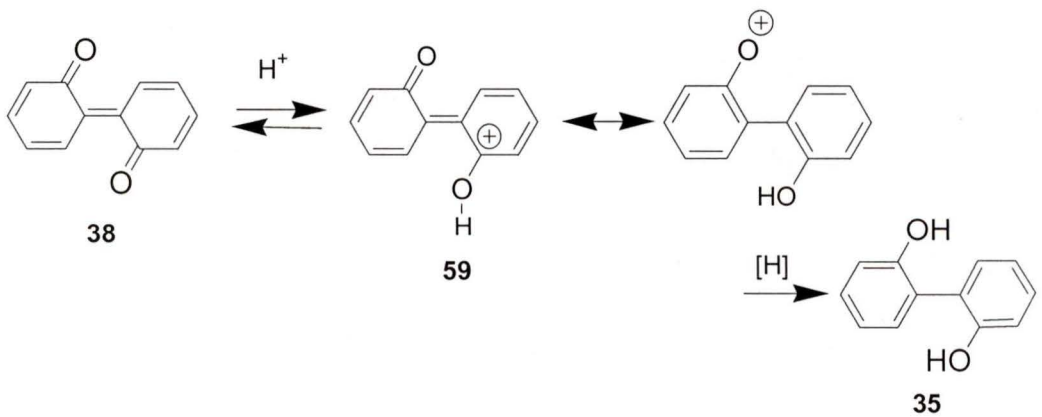

Scheme 2.4

2.3.3 Solvent Isotope Effects

The observation of a water-assisted reduction due to hydrogen bonding creates an interesting issue. Based on the data thus far, the organic solvents used have been proposed as the hydrogen donor in the reduction of the biphenylquinones to the biphenols. In particular, the comparison of decay lifetimes in CH_3CN and 2-propanol formed a conclusion that the solvent is participating directly in the reduction. The most recent evidence however suggests a water-assisted reduction through hydrogen bonding effects. If this is indeed the case, the possibility arises that the reduction in 2-propanol is also assisted through a similar hydrogen bonding effect. Because this assumption must be considered as a possibility, further studies had to be done to confirm the solvent's participation in the reduction. Therefore a solvent isotope study was launched in an effort to clarify the solvent's role in the reduction of the biphenylquinones.

An argon purged CH_3CN solution of **33** (3×10^{-4} M) was irradiated (300 nm) in a quartz cuvette for 30 s. A pink transient was generated and a UV-Vis spectrum was taken immediately after photolysis. The kinetics of the decay were monitored at 525 nm. An identical run was done in CD_3CN and the decay rate (k_D) measured was directly compared to the previous run (k_H). From these values the solvent kinetic isotope effect was calculated, by comparing the decay rate of **38** in CH_3CN to the decay rate in CD_3CN. The results revealed a primary kinetic isotope effect ($k_H/k_D = 1.93 \pm 0.04$). Identical studies were done to determine the solvent kinetic isotope effects of **39**, **40** and **41** based on the decay rates of their respective biphenylquinones in CH_3CN and CD_3CN. The results in Table 2.3 reveal a primary kinetic solvent isotope effect in all three derivatives.

These findings confirm that the solvent is participating in the reduction of the biphenylquinones in all the compounds studied. Once again the details of this reduction involve hydrogen abstraction from the solvent to give the respective biphenol as the final product.

Table 2.3 Solvent Isotope Effect on the Decay Rate of Biphenylquinones

Biphenylquinone	k_H (min^{-1})[a]	k_D (min^{-1})[a]	k_H/k_D
38	0.200 ± 0.01	0.104 ± 0.02	1.93 ± 0.2
51	0.521 ± 0.04	0.255 ± 0.03	2.04 ± 0.3
52	0.870 ± 0.05	0.412 ± 0.04	2.11 ± 0.2
53	0.212 ± 0.02	0.126 ± 0.02	1.68 ± 0.2

[a] Rates were calculated as an average of three separate trials

2.4 Laser Flash Photolysis (LFP) Studies

UV-Visible spectroscopy has provided major insight into the details of the photochemical mechanism of dibenzo-*p*-dioxins. In particular, the reduction of the biphenylquinones to the biphenols has been observed and the lifetimes of this conversion have been resolved. In order to provide further evidence of biphenylquinone formation upon photolysis of **33**, **39**, **40** and **41**, LFP studies were carried out using 266 nm and 308 nm excitations. These experiments were carried out in an attempt to observe the existence of the proposed spiroketone intermediate in both organic and aqueous solution.

Studies in acidic media were also carried out.

2.4.1 Observation of Transient Species

LFP (excimer laser, $\lambda_{ex} = 308$ nm, O_2 purged) of a CH_3CN solution of **33** gave two strong transients at 330 nm and 525 nm (Figure 2.8). The absorption band at 330 nm consisted of a first order decay with a measured lifetime of 238 ± 20 μs. The other band at 525 nm demonstrated first order growth which had a lifetime of 227 ± 20 μs. The transient at $\lambda_{max} = 330$ nm has been assigned as a reactive intermediate which decays into a new transient species at $\lambda_{max} = 525$ nm. This observed conversion of one reactive intermediate to another can be reasonably assigned as the conversion of the spiroketone **37** to the biphenylquinone **38**. The assignment of **38** as the transient observed at 525 nm is consistent with its absorption observed in previous UV-Vis studies (Figure 2.1). The transient decay observed at 330 nm has a similar lifetime to the growth of **38** and is therefore assigned as a reactive intermediate that serves as a precursor to the formation of **38**. The assignment of this transient as the spiroketone **37** is reasonable since this species would be expected to absorb in the 300-350 nm region. This assignment suggests that the growth and the decay traces observed are due to an electrocyclic ring-opening of the four-membered ring in the spiroketone **37** to yield the biphenylquinone intermediate **38**.

LFP (excimer laser, $\lambda_{ex} = 308$ nm, O_2 purged) of a 1:1 CH_3CN:H_2O solution of **33** revealed a spectrum with two strong transients similar to the ones described earlier. The lifetimes observed (Table 2.4) were very similar, suggesting that water does not have an effect on the rate of conversion from the spiroketone **37** to the biphenylquinone **38**.

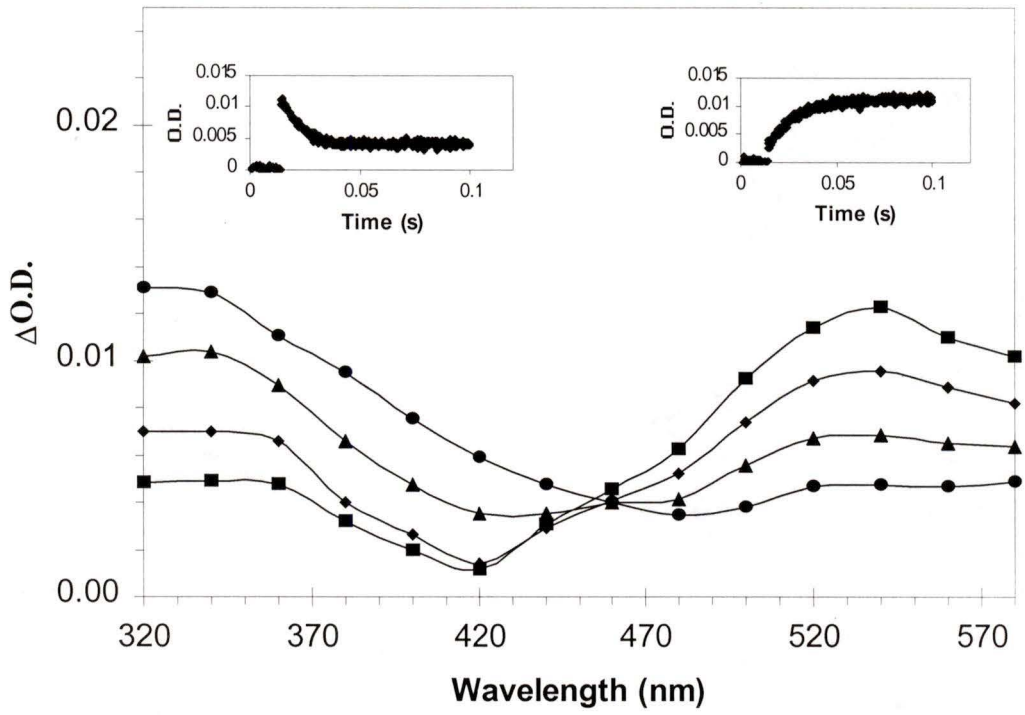

Figure 2.8 LFP spectrum of the photolysis **33** in dry CH_3CN, O_2 purged. Transient absorption at λ_{max} = 330 nm represents the decay of the spiroketone intermediate **37**. Absorption band at λ_{max} = 530 nm represents the growth of the biphenylquinone intermediate **38**. Left inset: Decay trace represents the disappearance of the spiroketone **37**. Right inset: Growth trace represents the formation of the biphenylquinone **38**.

LFP (excimer laser, λ_{ex} = 308 nm, O_2 purged) of an aqueous 1:1 CH_3CN-H_2O solution at pH 1 of **33** also gave two strong transients at 330 nm and 525 nm. The lifetimes were shown to decrease significantly in acidic media. The lifetime of biphenylquinone formation in neutral solution was measured at 227 ± 20 μs compared to a lifetime of 53 ± 6 μs in the presence of acid. This result suggests an acid-catalyzed ring-opening in the transition from the spiroketone **37** to the biphenylquinone **38.**

Table 2.4 Lifetimes of Biphenylquinone formation in various solvent systems.

Biphenylquinone	CH_3CN[a]	$CH_3CN:H_2O$ pH 7[a]	$CH_3CN:H_2O$ pH 1[a]
38	238 ± 20 μs	227 ± 20 μs	53 ± 6 μs

[a] Lifetimes were calculated as an average of three separate trials

This observation helps to provide some insight on the transition state of the ring-opening process of the spiroketone. The conversion involves a concerted electrocyclic ring-opening going through a charged transition state **61**. Scheme 2.6 illustrates a mechanistic justification for this described acid-catalysed ring-opening. Under acidic conditions protonation of the carbonyl oxygen of the spiroketone **37** is expected to occur to yield **60**. This will generate a positive charge on oxygen thus making the ring more electron deficient. Because of the electron deficiency in the ring, it is expected that heterolytic C-O bond cleavage would be favourable. This mode of cleavage would create the transition state **61** which bears a partial negative charge on the ring carbon and a partial positive charge on the oxygen. The generation of a negative charge on the previously electron deficient ring would be a favourable process brought on by the initial protonation in acidic media. This proposal on the nature of the transition state will be used further in the explanation of the substituent effects on the electrocyclic ring-opening process.

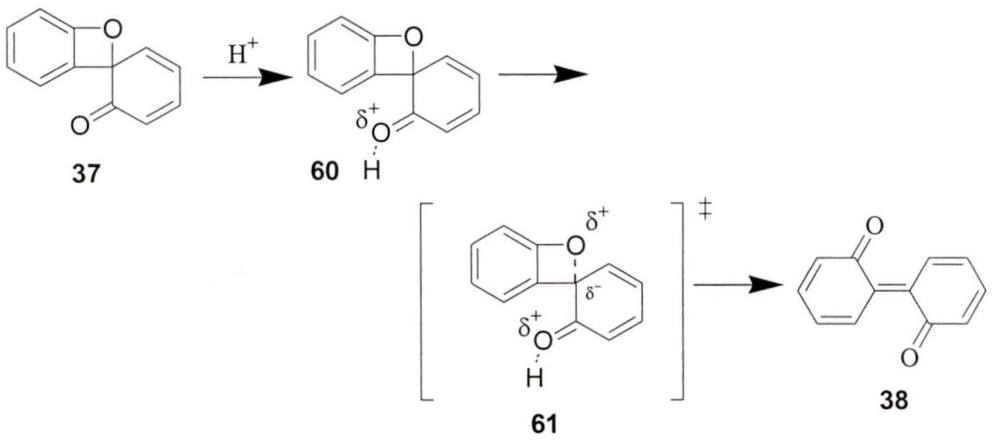

Scheme 2.6

LFP (excimer laser, λ_{ex} = 308 nm, O_2 purged) of a CH_3CN solution of **39** gave a strong transients at 560 nm (Figure 2.9). This observation is consistent with the UV-Vis spectrum of **43** shown earlier (Figure 2.2) . Because of this observation, the transient has been assigned as 4,4',5,5'-tetramethyl-2,2'-biphenylquinone (**43**). The LFP spectrum (Figure 2.9) is also consistent with the findings in the spectrum of the parent compound **33** (Figure 2.8) which has a large transient in the 500-550 nm region.

One major difference when comparing the LFP spectra of **33** and **39**, is the absence of the corresponding transient decay in Figure 2.7. An explanation for the absence of this transient may come from referring to the UV spectrum of **51** (Figure 2.2). This spectrum reveals two very strong absorption bands as a result of quinone formation (360 nm and 560 nm). It is believed that the strong absorption band observed at λ_{max} = 360 nm is directly affecting the appearance of the transient decay in the LFP spectrum (Figure 2.9). Because the lifetime of the quinone growth is equal the spiroketone decay lifetime it is reasonable to assume that these two bands are overlapping each other in the

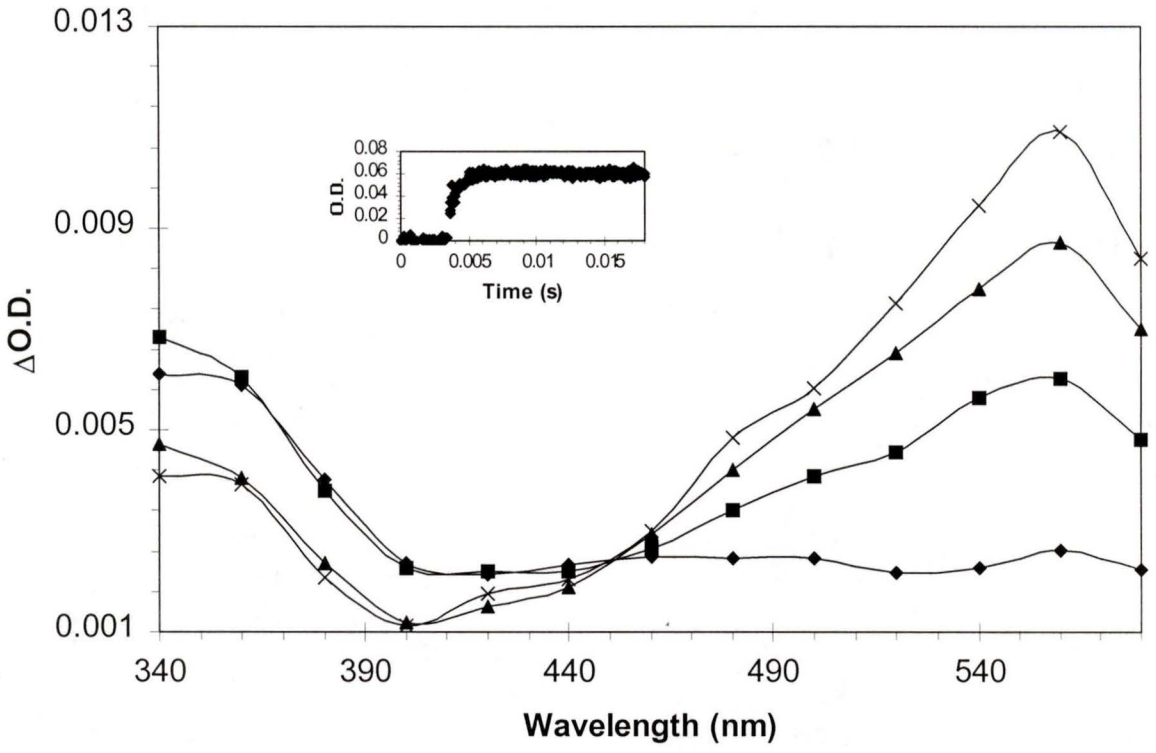

Figure 2.9 LFP spectrum of the photolysis **39** in dry CH_3CN, O_2 purged. Absorption band at λ_{max} = 530 nm represents the growth of the biphenylquinone intermediate **51**. Right inset: Growth trace illustrates the formation of the biphenylquinone **51**.

LFP spectrum in Figure 2.7. As a result, the transient cannot be readily discerned from the spectrum in Figure 2.9. A more important finding from this spectrum is the comparison of the lifetimes of the transient growth of **51** and **38** . The inset in Figure 2.9 suggests that the lifetime of biphenylquinone formation is much shorter in the photolysis of **39** than that observed in **33** (Figure 2.8). In order to understand this difference, it is necessary to reflect back to the nature of the transition state of the electrocyclic ring opening. As suggested earlier, the conversion of the spiroketone to the biphenylquinone, is expected to go through a charged transition state. This transition state involves

heterolytic cleavage of the C-O bond forming a partially charged species. Scheme 2.7 shows the transition state **62** with a partial positive charge residing on the oxygen and a partial negative charge residing on the ring carbon. Once again an understanding of the stability of this transition state is essential in the understanding of the substituent effect observed. The stabilities of these transition states can be compared by looking at the substituents on the aromatic ring. It is well known that methyl groups are good electron donors. The generation of a partial positive charge on the oxygen in **62** would take electron density away from the ring system. It is expected that methyl substituents would help out this deficiency by donating electron density to the electron deficient oxygen. Thus the transition state of the methylated complex would be the more favorable of the two, because its energy barrier would be lower than in the parent compound. It is also necessary to compare the stabilities of the biphenylquinones formed in each system. In both cases the mechanism involves the ring-opening of a spiroketone to form a biphenylquinone. This process involves going to a reactive intermediate that has two electron deficient ring systems. Because of this, it is expected that substituent effects will play a large part in the formation of a biphenylquinone complex. In comparing the two biphenylquinones (**38** and **51**) formed, it is obvious that the one bearing the methyl groups would be the more stable. Because of the electron donating effects of the methyl groups it is expected that they would help out the electron deficient rings in the system and thus **51** would be expected to be lower in energy and more stable than **38**. The observation that the lifetime of the formation of biphenylquinone **51** is faster than **38** is

then justified by not only its lower energy

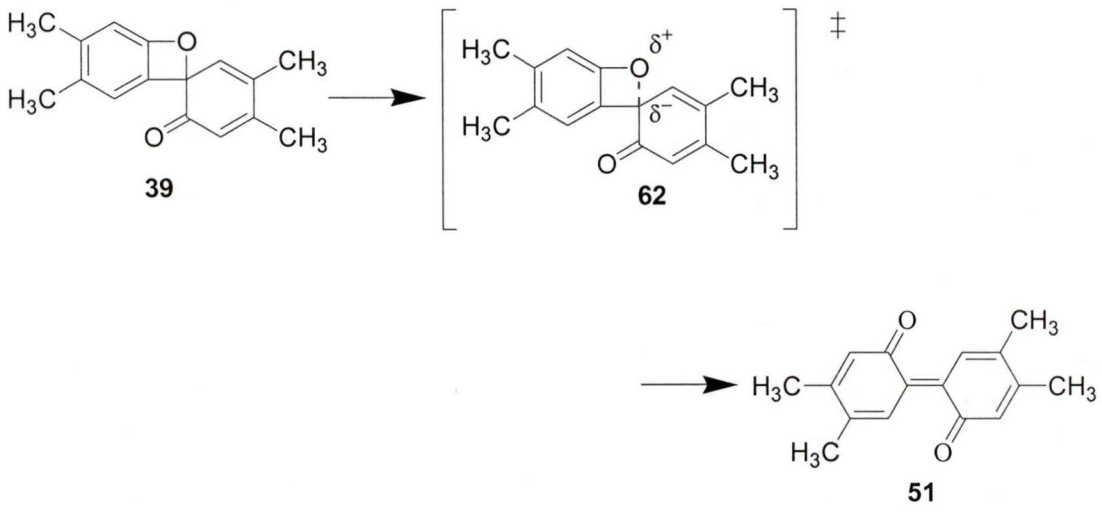

Scheme 2.7

transition state but also by the higher stability of the product formed.

The observations above suggests that the attachment of a better electron donating substituent will favor a faster ring-opening process. To test this hypothesis LFP (excimer laser, $\lambda_{ex} = 308$ nm, O_2 purged) of a CH_3CN solution of **40** was done and revealed no observable transients. The evidence presented thus far suggests that excitation of **40** should result in a very fast ring-opening that is aided by electron-donating substituents. Because a methoxy substituent is considered a better electron donor than any of the others substituents being studied, it is expected that the lifetime of the growth of **52** will be shorter than that observed for **51** ($\approx$ 9 μs). The spectra obtained for **40** suggests that this may indeed be the case. The absence of any transient species in the LFP spectra may suggest that the ring-opening is more rapid than the detection limits of our laser system

meaning that it occurs within the laser pulse (< 50 ns).

LFP (excimer laser λ_{ex} = 308 nm, O_2 purged) of a CH_3CN solution of **41** gave a strong transients absorption at λ_{max} = 540 nm (Figure 2.10). The lifetime of this transient was calculated to be ≈ 16μs. The observation of this transient was consistent once again with the UV-Vis spectrum (Figure 2.4) of 5,5'-difluoro-2,2'-biphenylquinone**53** and thus it has been assigned as the formation of this reactive intermediate. Comparing its lifetime with the other observed measurements (Table 2.5) provides more insight into the details of this mechanism. As expected the lifetime of **53** was longer than those observed in the formation of **51** and **52**. It was determined earlier that electron donating substituents

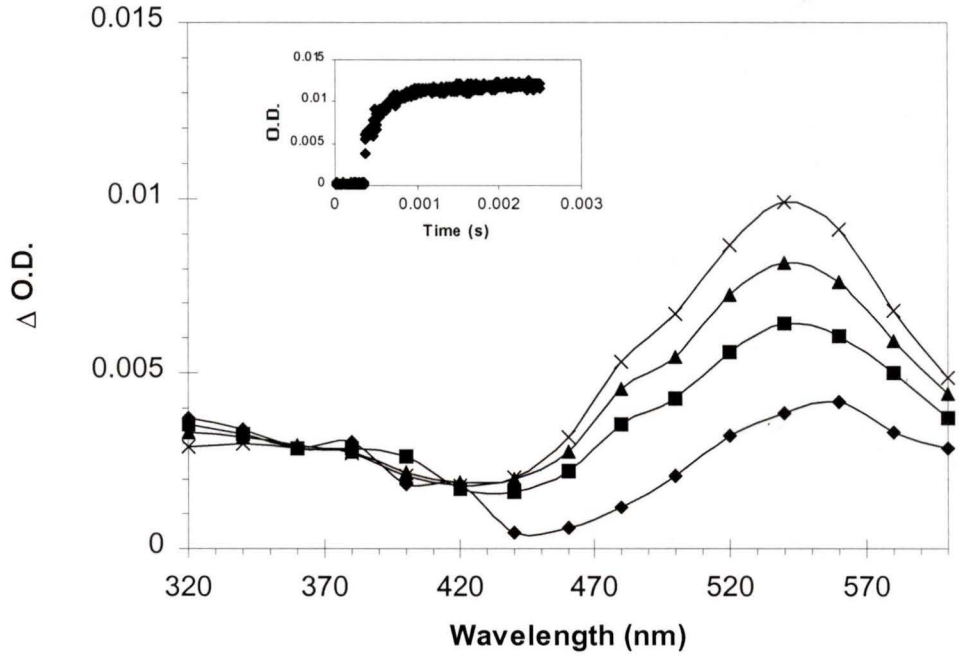

Figure 2.10 LFP spectrum of the photolysis **41** in dry CH_3CN, O_2 purged. Transient absorption at λ_{max} =560 nm represents the growth of the biphenylquinone intermediate **53**. Inset: Growth trace illustrates the formation of the biphenylquinone **53**.

Table 2.5 Observed Lifetimes of Biphenylquinone formation in CH_3CN

Biphenylquinone	k (s^{-1})	Lifetimes (μs)[a]
38	$4.2 \times 10^3 \pm 0.3$	240 ± 20
51	$1.1 \times 10^5 \pm 0.2$	9 ± 2
53	$6.2 \times 10^4 \pm 0.9$	16 ± 3

[a] Lifetimes were calculated as an average of three separate trials

enhance the rate of ring-opening. Based on this finding it seems logical that electron-withdrawing substituents should generate the opposite effect. The observation of a longer lifetime in the fluorinated system defends this idea. Mechanistically it is expected that formation of biphenylquinone **53** would be less favored due to the electron withdrawing nature of its fluorine substituents. As mentioned earlier the biphenylquinone system is already electron deficient, thus the addition of fluorine substituents should take even more electron density from the ring moiety. Because of this effect, the observation of an increased lifetime in the formation of **53** is anticipated. A comparison of the transient lifetimes of **53** with those observed in the parent system **33** (Table 2.5) reveal that the lifetime of formation is shorter in the fluorinated system. In other words, ring-opening of the fluorinated spiroketone **63** is a more favorable process than in the parent system. Once again this substituent effect can be justified by comparing the relative energies of the charged transition states. Scheme 2.8 illustrates the fluorine atom's participation in the stabilization of the partial negative charge in the transition state. Because fluorine is

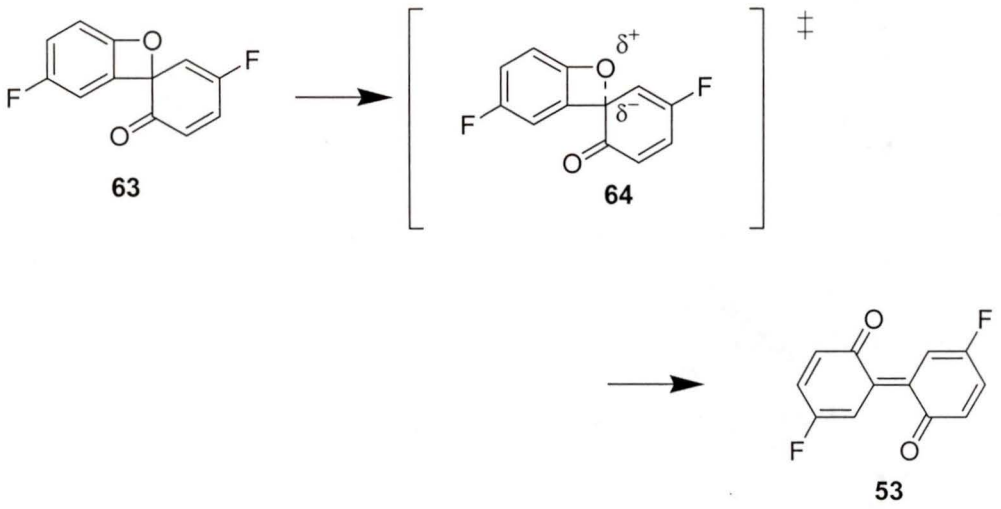

Scheme 2.8

an electron acceptor it can stabilize this transition state **64** more efficiently than a hydrogen subsitituent in the parent system. This effect will be expected to lower the energy in the transition state resulting in a more efficient reaction (shorter lifetime).

The Hammett plot shown in Figure 2.11 illustrates the effects substituents have on the system. Log k vs. the sum of the Hammet substituent constants ($\sigma^+$and σ^-) reveals a linear plot with a negative slope value. The sign of the slope, otherwise known as ρ, indicates that the reaction centre becomes more electron poor in the transition state as compared to the starting material. Therefore, because of the nature of the transition state electron donating substituents are expected to enhance the rate of reaction. This result is consistent with the proposed transition state of electrocyclic ring-opening. It should be mentioned that the transition state invokes two oppositely charged species. A positive charge is generated on the oxygen while a negative charge is formed on the ring carbon.

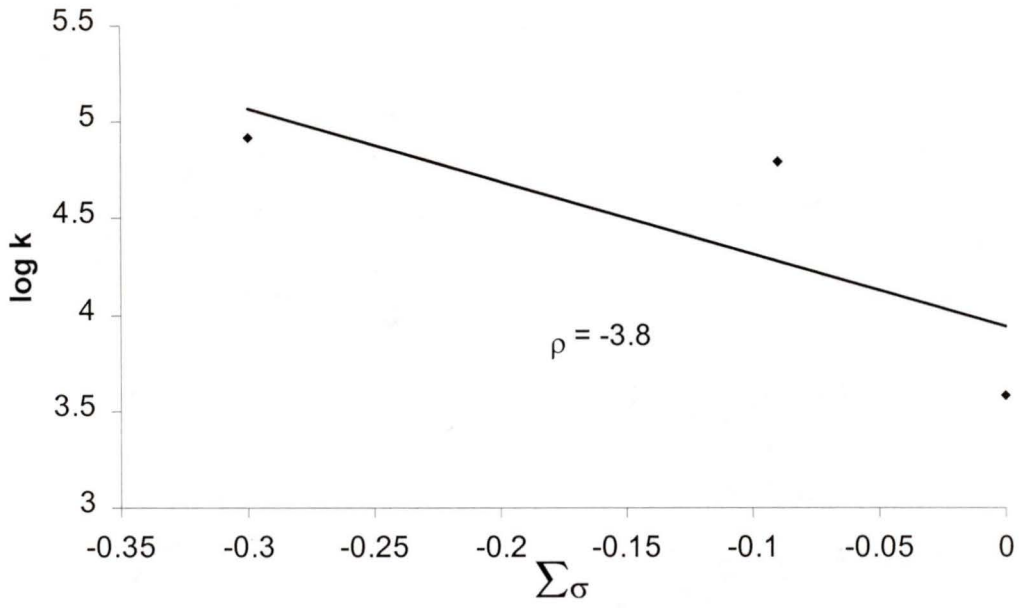

Figure 2.11 Hammet plot of log k (rates of biphenylquinone formation) versus the sum of σ^+ and σ^- illustrating the substituent effects on biphenylquinone formation.

The Hammet plot and the magnitude of its ρ value (-3.76) suggests that the sensitivity of the reaction is based strongly on the electron deficient site. Therefore the stabilization of the positive charge on oxygen determines the efficiency of the ring-opening process. Extrapolation of the Hammett plot in figure 2.11 suggests that the lifetime of the 5,5'-dimethoxy-2,2'-biphenylquinone formation would be shorter than those observed for the other three species. This observation is consistent with the assumption that a lack of transient absorptions in the LFP spectrum of **38** was due to the time scale limitations of the laser system used.

2.5 Summary

A mechanism for the photochemical decomposition of dibenzo-*p*-dioxin (**33**) and three of its derivatives (**39**, **40**, and **41**) has been proposed (Scheme 2.8). The results presented in this thesis have suggested a generalized photochemical mechanism for these types of compounds. The mechanism involves aryl-oxygen bond homolysis of the initial ring system to generate the singlet biradical **34**. This species can recombine to give starting material or undergo intramolecular ipso attack on the adjacent phenyl ring to generate the spiroketone intermediate **37.** Alternatively, the biradical can also abstract hydrogen from solvent forming the 2-phenoxyphenol (**6**) but this is a minor product. Due to ring strain and steric bulk of the spiroketone system, electrocyclic ring-opening follows generating a 2,2'-biphenylquinone intermediate (**38**). The lifetime of this ring-opening process was resolved using laser flash photolysis techniques and was found to be enhanced in acidic media. In addition, the presence of electron-donating subtituents were found to enhance this process. The observation of the biphenylquinone intermediates was achieved by UV-visible spectroscopy and their lifetimes were determined in various solvent systems. The reduction was enhanced in both water and acid. Primary kinetic isotope effects revealed that **25** could be reduced by solvent to yield 2,2'-biphenol (**35**) as the major photoproduct of this system.

The photoreactions of **37**, **38**, and **39** provide results that suggest that these derivatives react via the same mechanism that has been proposed for the parent system. The conversion of the spiroketone **37** to the biphenylquinone **38** was favored in the compounds with electron-donating substituents. UV-Vis spectra were obtained for all the

2,2'-biphenylquinone intermediates and their corresponding lifetimes were calculated. All compounds studied revealed the presence of a 2,2'-biphenol as the major photochemical product.

It is anticipated that this mechanism could be operative in the photochemistry of the notorious 2,3,7,8-tetrachlorodibenzo-*p*-dioxin (**27**). The decomposition of this compound is of intense interest and the findings in this Thesis should provide a strong framework for understanding the mechanistic photochemistry of this system.

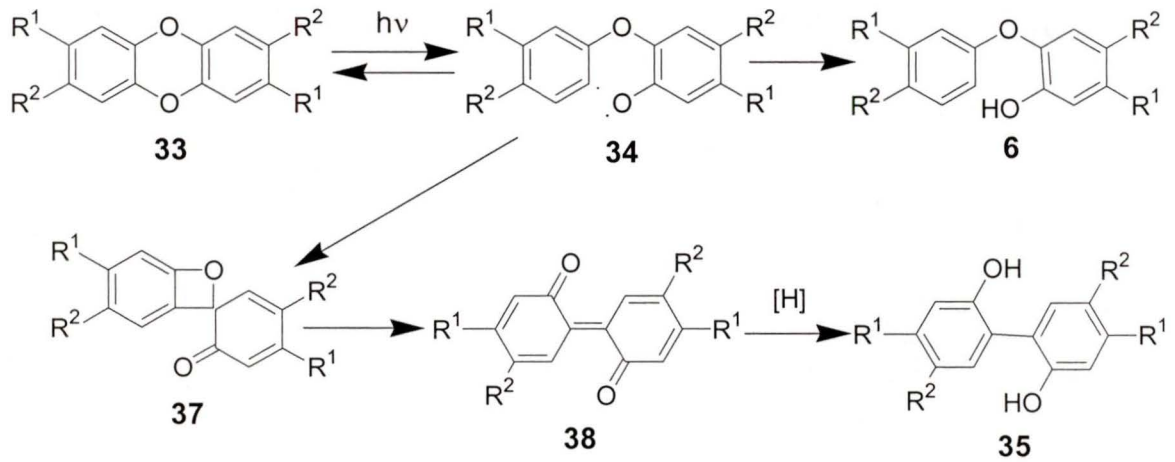

33 R^1 and R^2 = H

39 R^1 and R^2 = CH_3

40 R^1 = OCH_3, R^2 = H

41 R^1 = F, R^2 = H

Scheme 2.9

Chapter 3

Experimental

3.1 Instrumentation

^{1}H NMR spectra were recorded on either a Bruker AC 300 (300 MHz), AM 360 (360 MHz), or a AMX 500 (500 MHz) instrument using $CDCl_3$, CD_3CN, or acetone-d_6 as solvent. Chemical shifts were reported in ppm downfield from 0 (determined from the residual solvent signal). Splitting patterns were reported as a s (singlet), d (doublet), t (triplet) and q (quartet). Mass spectra were determined on a Finnegan 3300 (CI) or a Kratos Concept 1H (EI and HRMS). Transient UV-Vis spectra and kinetic measurements were recorded using nanosecond LFP with excitation by either a Spectra Physics YAG laser (Model GCR-12, 266 nm excitation) or a Luminocs excimer laser (Model EX-510, 308 nm excitation). UV-vis spectra and kinetic experiments were recorded using a Varian Cary 50 Bio instrument. Melting points were taken on a Gallenkamp apparatus and are uncorrected. Preparative thin layer chromatography (TLC) was performed on 1000 μm silica gel plates from Analtech and the solvent systems used are listed in the individual experiments. Analytical TLC was performed on Machery-Nagel PolygramSIL/UV_{254} silica gel plates. pH was measured with a Corning 140 pH meter. Preparative photolyses were performed in a Rayonet RPR 100 photochemical reactor using 300 nm lamps with 100 mL quartz tubes. Small scale UV-Vis experiments were performed in 3 mL Suprasil quartz cuvettes.

3.1.1 Laboratory Reagents and Solvents

HPLC grade acetonitrile was distilled over CaH_2 for use in UV, photolysis and LFP studies. Reagent grade dichloromethane was distilled before use. 95% Ethanol, spectra grade methanol and isopropanol were used as received. Solutions of specific pH were made up with aqueous NaOH and H_2SO_4.

3.2 Synthesis

The synthesis of **33** was not performed as it was available in the lab from an earlier study. The identity of the product was checked for purity by m.p. and ^{1}H NMR. All reagents utilized for synthesis were purchased from Aldrich and were also used after subsequent purity checks.

2,3,7,8-Tetramethyldibenzo-*p*-dioxin (37)

The adapted synthesis was based on the procedure of Tomita.[38] 2-Chloro-4,5,-dimethylphenol (5 g, 0.03 mole), anhydrous K_2CO_3 (2 g, 0.015 mole) and copper powder (0.25 g) were heated under N_2 in a sand bath at 190-250°C for 10 h. The hard, ground up mixture was then refluxed under N_2 with 25 mL of 5M K_2CO_3 solution for 2 h. The product mixture was extracted with CH_2Cl_2, and the organic portion was washed with 2 M KOH (3 × 100 mL). Evaporation of CH_2Cl_2 gave crude product, which was recrystallized in methanol resulting in pure **37** as a white powder (0.21g, 5 %), m.p. 167-169°C (lit [38] m.p. 167°C); MS *m/z* =241 (M^+ + 1); ^{1}H NMR (360 MHz, $CDCl_3$) δ 2.11 (12H, s, CH_3), 6.59 (4 H, s, Ar-H).

2,7-Dimethoxydibenzo-*p*-dioxin (40)

An adapted procedure for the synthesis of **37** was used. 2-Chloro-4-methoxyphenol (5 g, 0.03 mole), anhydrous K_2CO_3 (2 g, 0.015 mole) and copper powder (0.25 g) were heated under N_2 in a sand bath at 190-250°C for 14 h. The black solid was then refluxed under N_2 with 25 mL of 5M K_2CO_3 solution for 2 h. The product mixture was extracted with CH_2Cl_2, and the organic portion was washed with 2M KOH (3 × 100 mL). Evaporation of CH_2Cl_2 gave crude product, which was recrystallized in methanol resulting in pure **40** as white needles. (0.05g, 1.3 %), m.p. 167-169°C; HRMS (EI) Calc. $C_{14}H_{12}O_4$: 244.0735, found: 244.0739. ^{1}H NMR (300 MHz, acetone-d_6) δ 3.75 (6H, s, OCH_3), 6.48 (2H, d, J=3, H 2 and 6), 6.50 (2H, dd, J=8 and 3 Hz, H-4 and H-8), 6.83 (2H, d, J=8, H-5 and H-9). ^{13}C NMR (300 MHz, acetone-d_6) δ 56.0 (OCH_3), 103.1 (C-2 and C-8), 109.3 (C-4 and C-10), 117.3 (C-5 and C-11), 136.2 (C- 6 and C-12), 143.4 (C-1 and C-7) and 157. 2 (C-3 and C-9).

2,7-Difluorodibenzo-*p*-dioxin (41)

An adapted procedure for the synthesis of **37** was used. 2-Chloro-4-fluorophenol (5g, 0.02 mole), anhydrous K_2CO_3 (2g, 0.015 mole) and copper powder (0.25g) were heated under N_2 in a sand bath at 190-250°C for 8 h. The black solid material was then refluxed under N_2 with 25 mL of 5 M K_2CO_3 solution for 2 h. The product mixture was extracted with CH_2Cl_2, and the organic portion was washed with 2 M KOH (3 × 100 mL). Evaporation of CH_2Cl_2 gave crude product, which was sublimed under reduced pressure resulting in pure **41** as white needles. (2.1 g, 66 %): m.p. 174-176°C (lit [40] m.p. 174-

176°C); HRMS (EI) Calc. $C_{12}H_6O_2F_2$: 220.0336, found: 220.0337. ^{1}H NMR (500 MHz, $CDCl_3$) δ 6.58 (4H, d, J = 9 and 3 Hz, H-1 and H-6,), 6.60 (2 H, dd, J =9 and 3 Hz, H-3 and H-8) and 6.77 (2H, d, J=8 and 6 Hz, H-4 and H-9). ^{13}C NMR (300 MHz, acetone-d_6) δ 105.1 (C-2 and C-8), 111.2 (C-4 and C-10), 117.8 (C-5 and C-11), 158.1 (C- 6 and C-12), 161.2 (C-1 and C-7) and 169.3 (C-3 and C-9).

3.3 Product Studies

All preparative photolyses were done in a Rayonet RPR 100 photochemical reactor equipped with 254 or 300 nm lamps depending on the experiment done. Samples (20 -100 mg) were dissolved in aqueous or dry CH_3CN and transferred to a 100 mL quartz tube. The solution was cooled (≈ 18°C) and argon purged for about 20 minutes before photolysis and continued throughout irradiation. The length of photolysis varied depending on the efficiency of the photochemical reaction.

The workup of the reactions in dry organic solvents was done by evaporation of the solvent. In aqueous solution a saturated solution of NaCl was added and the products were extracted with CH_2Cl_2. The extracts were dried over $MgSO_4$ and then filtered. Evaporation of the CH_2Cl_2 provided the crude products of the photoreaction. Separation of the mixture was achieved through preparative thin layer chromatography. Once separated the products were characterized by ^{1}H and ^{13}C NMR, MS and m.p.

Photolysis of Dibenzo-*p*-dioxin (33) in Dry CH_3CN

A 50 mg sample of **33** was dissolved in 80 mL of dry CH_3CN solution in a quartz

tube. The cooled (≈ 18 °C), argon purged solution was irradiated at 300 nm for 40 min. Evaporation of the solvent gave a dark brown crude product. ^{1}H NMR integration analysis of the crude product allowed observation of 21% conversion to one major photoproduct **35**. The major product was separated from the mixture using preparative TLC (silica gel, CH_2Cl_2; R_f, 0.19 (**35**), 0.73 (**33**). The product was identified by ^{1}H NMR and compared to an authentic compound which is commercially available.

Photolysis of Dibenzo-*p*-dioxin (33) in 1:1 H_2O-CH_3CN (pH 7)

A 50 mg sample of **33** was dissolved in 80 mL of 1:1 H_2O-CH_3CN (pH 7) solution in a quartz tube. The procedure described above was followed. ^{1}H NMR integration analysis of the crude product allowed observation of 21% conversion to one major photoproduct **35**. The major product was separated from the mixture using preparative TLC (silica gel, CH_2Cl_2; R_f, 0.19 (**35**), 0.73 (**33**). The product was identified by ^{1}H NMR and compared to an authentic compound which is commercially available.

Photolysis of Dibenzo-*p*-dioxin (33) in 1:1 H_2O-CH_3CN (pH 1)

A 50 mg sample of **33** was dissolved in 80 mL of 1:1 H_2O-CH_3CN (pH 1) solution in a quartz tube. The cooled (≈ 18 °C), argon purged solution was irradiated at 300 nm for 40 min. Following photolysis, 100 mL of saturated NaCl solution was added and the solution was extracted with 3 × 100 mL CH_2Cl_2. The extracted solutions were combined and dried over $MgSO_4$, filtered and evaporated to dryness. ^{1}H NMR

integration analysis of the crude product allowed observation of 21% conversion to one major photoproduct **35**. The major product was separated from the mixture using preparative TLC (silica gel, CH_2Cl_2; R_f, 0.19 (**35**), 0.73 (**33**). The product was identified by ^1H NMR and compared to an authentic compound which is commercially available.

Photolyses of **33** in aqueous solutions were done at various pH (1-12) using the same procedure explained above. The results revealed no significant changes in the efficiency of the photoreaction with respect to pH. The pH's of the solutions were adjusted using concentrated NaOH and H_2SO_4 solutions.

Photolysis of 2,7-Difluorodibenzo-*p*-dioxin (41) in dry CH_3CN

A 50 mg sample of **41** was dissolved in 80 mL of CH_3CN solution in a quartz tube with 5 mg of $NaBH_4$. The cooled (≈ 18°C), argon purged solution was irradiated at 300 nm for 2 hrs. Evaporation of the solvent gave a grey crude product. ^1H NMR integration analysis of the crude product allowed observation of 40% conversion to one major photoproduct **43**. The major product was separated from the mixture using preparative TLC (silica gel, 80:2 hexanes:ether R_f, 0.23 (**41**), 0.79 (**39**). m.p. 120°C, HRMS (EI) Calc. $C_{12}H_8O_2F_2$: 222.0492, found: 244.0496. ^1H NMR (500 MHz, acetone-d_6) δ 6.99 (2H, d, J = 9.5, $c_{3,3'}$-H), 7.01 (2 H, dd, J = 8 and 3 Hz, $c_{4,4'}$-H), 7.07 (2H, d, J = 9.5, $c_{6,6'}$-H) and 8.43 (2H, s, Ar-OH, exchangeable with D_2O). ^{13}C NMR (300 MHz, acetone-d_6) δ 115.2 (C-4 and C-4', C-6 and C-6'), 118.2 (C-3 and C-3'), 127.8 (C-1 and C-1'), 150.1 (C-2 and C-2') and 155.5 (C-5 and C-5').

Photolysis of 2,7-Dimethoxydibenzo-*p*-dioxin (40) in dry CH_3CN

A 15 mg sample of **40** was dissolved in 80 mL of CH_3CN solution in a quartz tube with 5 mg of $NaBH_4$. The cooled (≈ 18°C), argon purged solution was irradiated at 300 nm for 2 hrs. Evaporation of the solvent gave a brown crude product. ^1H NMR integration analysis of the crude product allowed observation of 40% conversion to one major photoproduct **42**. The major product was separated from the mixture using preparative TLC (silica gel, 1:1 hexanes:ether R_f, 0.21 (**42**), 0.83 (**40**). m.p. 126°C (lit.[41] m.p.127°C), HRMS to be reported. ^1H NMR (500 MHz, acetone-d_6) δ 6.83 (2H, d, J = 3 Hz, $c_{6,6'}$-H), 6.84 (2 H, dd, J = 8 and 3 Hz, $c_{4,4'}$-H), 6.91 (2H, d, J = 8 Hz, $c_{3,3'}$-H) and 8.31 (2H, s, Ar-OH, exchangeable with D_2O). ^{13}C NMR (300 MHz, acetone-d_6) δ 115.2 (C-4 and C-4', C-6 and C-6'), 118.2 (C-3 and C-3'), 127.8 (C-1 and C-1'), 150.1 (C-2 and C-2') and 155.5 (C-5 and C-5').

3.3.1 Dark Reactions

Compounds **33** and **39-41** were allowed to sit in the dark for several hours in all solvent systems tested. Following the standard work up, no reaction was observed in any of the cases.

3.4 Characterization of 2,2'-Biphenylquinones

3.4.1 UV-Vis Studies

UV-Vis studies were done by direct photolysis of the solutions in a UV cuvette.

Stock solutions were prepared by dissolving 20 mg of sample in 3 mL of the appropriate solvent. Small amounts of the stock solution (5 -20 μL) were injected into a quartz cuvette containing 3 mL of solvent. The samples were purged with argon for 5 minutes and sealed with a Teflon cap. A copper wire cage was designed to lower the cuvettes into a photoreactor with an internal cooling fan. The cuvette was dangled inside the reactor and was irradiated for 30 s at 300 nm. Baselines were measured on the UV-Vis instrument before photolyses were performed. UV spectrums were run immediately after photolysis. Rate constants and lifetimes were measured three times and the average of these trials were calculated for each species.

Observation of 2,2'-Biphenylquinone (38)

An argon purged, dry CH_3CN solution of **33** (3×10^{-5}M) in a quartz cuvette was irradiated at 300 nm for 30 s. The resulting pink solution was immediately removed from the photoreactor and a UV spectrum was recorded. Two new absorption bands formed at λ_{max} 345 and 532 nm and have been assigned as biphenylquinone **38**. The decay of the bands were monitored by identical methods over time in different solvent systems.

Observation of 4,5,4',5'-Tetramethyl-2,2'-biphenylquinone (51)

An argon purged, dry CH_3CN solution of **39** (3×10^{-5}M) in a quartz cuvette was irradiated at 300 nm for 30 s. The resulting pink solution was immediately removed from the photoreactor and a UV spectrum was recorded. Two new absorption bands formed at

λ_{max} 353 and 566 nm and have been assigned as biphenylquinone **51**. The decay of the bands were monitored by identical methods over time in different solvent systems.

Observation of 5,5'-Dimethoxy-2,2'-biphenylquinone (52)

An argon purged, dry CH_3CN solution of **40** (3×10^{-5}M) in a quartz cuvette was irradiated at 300 nm for 30 s. The resulting blue solution was immediately removed from the photoreactor and a UV spectrum was recorded. A new absorption band was formed at λ_{max} = 620 nm and has been assigned as biphenylquinone **52**. The decay of this species was monitored over time in different solvent systems.

Observation of 5,5'-Difluoro-2,2'-biphenylquinone (53)

An argon purged, dry CH_3CN solution of DFBD (**41**) (3×10^{-5}M) in a quartz cuvette was irradiated at 300 nm for 30 s. The resulting pink solution was immediately removed from the photoreactor and a UV spectrum was recorded. A new absorption band was formed at λ_{max} 520 nm and has been assigned as biphenylquinone **53**. The decay of this species was monitored over time in different solvent systems.

3.4.2 Solvent Isotope Effect

Solvent Isotope Effects on the Decay Rates of 38, 51, 52, 53

Irradiation of an argon purged dry CH_3CN or CD_3CN solution of **33** (3×10^{-5}M) at ambient temperature in a quartz cuvette for 30 s revealed a pink transient whose UV

spectrum was recorded immediately. The absorbance band at 532 nm was monitored at 30 s intervals until it decayed to baseline. Rate constants and lifetimes were calculated from this data and the results of the CH_3CN solutions were directly compared with CD_3CN solutions. The isotope effect was determined by the rate data to be $k_H/k_D = 1.93 \pm 0.08$. Identical experiments were done on the decay of the reactive intermediates **51**, **52** and **53** and all revealed similar primary kinetic isotope effects.

3.4.3 Laser Flash Photolysis (LFP) Studies

All LFP experiments were done in the LFP Facility at the University of Victoria. Depending on the nature of the experiment and the species studied, spectral and kinetic measurements were done using a Nd:YAG laser (Spectra Physics Quanta-Ray, GCR-12) at an excitation wavelength of 266 nm. Experiments were also done using a Lumonics excimer laser (Model EX-510, 308 nm excitation). In an attempt to avoid possible multiphoton effects, pulse energies were adjusted to < 20 mJ/pulse. The monitoring light source was am 150 W pulsed Osram lamp Model XBO 150W-1 with Oriel housing Model 66057 and a PTI power supply LPS-220. In order to measure the growth and decay for longer lived transients ($\tau > 10$ μs), the pulser was turned off. For all experiments, minimization of laser interference was accomplished by angling the monitoring lamp and the detection equipment 90° to the laser beam. Light intensity at individual wavelengths was detected using a CVI Digikrom 240 monochromator and a Hamamatsu R446 (5 dynodes) photomultiplier tube (PMT). PMT signals were transmitted to a baseline compensation unit. Signals resulting from laser firing were

recorded using the Tektronix TDS 520 digital oscilloscope and sent to the computer system. Baseline correction was necessary where the time scale observed was above 5 μs/div. The software Labview 5.01was used on a MacIntosh G3 to run the laser system.

For all experiments the P_0 values were maintained between -0.185V and -0.250V. In cases where the monitoring lamp pulser was turned on, the PMT voltage and monochromator slit width was adjusted automatically. In experiments where longer time scales ($\tau > 10$ μs) were studied and the lamp pulser was turned off, the PMT voltage and monochromator slit width was adjusted manually.

All laser experiments were done in a flow cell with rubber tubing which ran through a mechanical pump to control the solvent flow rate. The solution being analysed was purged in the flow cell for 20 min before the beginning of the experiment and was continued until the end of the experiment. In all cases the purging was done with either nitrogen or oxygen gas.

Optical densities of about 0.3 were achieved in a particular solvent system by adjusting the concentration of the solution from an initial stock solution. Equation 4.5 was implemented to determine the volume of the stock solution required to make up the substrate solution (80-100mL) to be analysed.

$$SV = (0.3\ S / Abs)\ (10/7)\ (x / 3 + s) \qquad (4.1)$$

Where: SV = Spike volume (in μL) required to yield an O.D. of 0.3 in x mL

S = Volume of spike (in μL) used to give O.D. of ~ 0.3 in cuvette

Abs = Absorbance measured from the spike of S μL in a 3 mL cuvette

x = Volume of solvent required in the flow cell (typically 80 - 100mL)

s = Volume of spike in mL

10/7 = ratio of path length for the cuvette and flow cell

Laser spectra consisted of a collection of ΔO.D. measurements from all the monitoring wavelengths. Experiments consisted of 7 - 15 laser shots at each wavelength monitored. The experiments were followed through four monitoring windows, each of which consisted of a transient signal at different time frames. Transient decays and growths were recorded as a collection of 500 time resolved points at a specific wavelength at a given time scale. The decays and growths were fitted using a Labview program written for the University of Victoria LFP facility (FitVic).

References

1. H. J. Hageman, H. L. Louwerse and W. J. Mus, *Tetrahedron,* **1970**, 26, 2045.

2. A. Norstrom, K. Anderson and C. Rappe, *Chemosphere*, **1976**, 1, 21.

3. G. G. Choudry, G. Sundstrom, F. Van der Wielen and O. Hutzinger, *Chemosphere*, **1977**, 6, 327.

4. C. G. Huang, D. Shukla and P. Wan, *J. Org. Chem.*, **1991**, 56, 5437.

5. M. S. Kharasch, G. Stampa and W. Nadenberg, *Science,* **1952**, 116, 309.

6. F. L. Bach and J. C. Barclay, *Abstract of Papers, 150th meeting of the American Chemical Society,* **1965**, 95.

7. Y. Ogata, K. Takayagi and I. Ishino, *Tetrahedron*, **1970**, 26, 2703.

8. H. I. Joschek and S. I. Miller, *J. Am. Chem. Soc.,* **1966**, 88, 3269.

9. N. Haga and H. Takayanagi, *J. Org. Chem.*, **1996**, 61, 735.

10. J. A. Elix and D. P. Murphy, *Australian J. Chem.,* **1975**, 28, 1559.

11. B. Guan and P. Wan, *J. Photochem. Photobiol. A: Chem.,* **1994**, 80, 199.

12. F. R. Hewgill and D. G. Hewitt, *J. Chem. Soc. (C),* **1967**, 723.

13. H. D. Becker and K. Gustafsson, *Tetrahedron Lett.*, **1976**, 55, 4883.

14. F. R. Hewgill, *Tetrahedron*, **1978**, 34, 1595.

15. E. A. Braude, C.E. Jackman and R. P. Linstead, *J. Chem. Soc.,* **1954,** 3548.

16. E. S. Lewis, J. M. Perry and R. H. Grinstein, *J. Am. Chem. Soc.,* **1970**, 92, 899.

17. S. H. Burnstein and H. J. Ringold, *J. Am. Chem. Soc.,* **1964**, 86, 4952.

18. D. D. Reid, M. Fraser, B. B. Molloy, H. A. S. Payne and R. G. Sutherland, *Tetrahedron Letters,* **1961,** 530.

19. O. Neunhoeffer and P. Heitman, *Chem. Ber.,* **1963,** 96, 1027.

20. A. S. Hay, *Tetrahedron Letters,* **1965,** 47, 4241.

21. H. D. Becker, *J. Org. Chem.*, **1965**, 30, 989.

22. J. H. Exner, J. D. Johnson, O. D. Ivins, M. N. Wass and R. A. Miller, "*Detoxication of Hazardous Wastes*", H. Exner (ed.), Ann Arbor Science Publishers, Ann Arbor , **1982**

23. A. J. Dobbs and C. Grant, *Nature,* **1978**, 278, 163

24. N. Kimura and Y. Urushigawa, *Journal of Bioscience and Bioengineering,* **2001**, 92, 138.

25. R. Pollard and P. Wan, *Org. Prep. Proc. Int.* **1993**, 25, 1.

26. D. G. Crosby, A. S. Wong, J. R. Plimmer and E. A. Woolson, *Science,* **1971**, 173, 748.

27. A. J. Dobbs and C. Grant, *Nature,* **1979**, 278, 163.

28. H. R. Buser, *Chemosphere*, **1979**, 8, 251.

29. A. Mamantov, *Chemosphere,* **1985**, 14, 897.

30. G. A. Epling, Q. Qiu and A. Kumar, *Chemosphere,* **1989,** 18, 329.

31. G. G. Choudry, G. R. Webster, *J. Agric. Food Chem.,* **1989**, 37, 254-261.

32. D. Dulin, H. Drossman, and T. Mill, *Environ. Sci. Technol.,* **1986**, 20, 72.

33. A. D. Konstantinov, A. M. Johnston, B. J. Cox, J. R. Petrulis, M. T. Orzechowski and N. J. Bunce, *Environ. Sci. Technol.,* **2000**, 34, 143.

34. S. Kieatiwong, L. V. Nguyen, V. R. Hebert, M. Hackett, G. C. Miller, M. J. Millie and R. Mitzel, *Environ. Sci. Technol.,* **1990**, 24, 1575.

35. S. Rayne, P. Wan, M. G. Ikonomou and A. D. Konstantinov, *Environ. Sci. Technol.,* **2002**, 36, 1995.

36. J. R. Plimmer, U. I. Klingerbiel, D. G. Crosby and A. S. Wong, "*Advances in Chemistry Series*", E.H. Blair (ed.), American Chemical Society, Washington, **1973**, 120, p.44.

37. R. Masse and B. Pelletier, *Chemosphere,* **1987**, 16, 7.

38. M. Tomita, *J. Pharm. Soc. Jpn.,* **1933**, 53, 775.

39. H. Gilman and J. J. Dietrich, *J. Am. Chem. Soc.,* **1957**, 79, 1439.

40. W. Mailahn U. Haffer and W. Rotard, *Chemosphere.,* **1994**, 29, 1803.

41. G. Sartori, R. Maggi, F. Bigi, A. Attilio and G. Casnati, *Tetrahedron.*, **1992**, 43, 9483.

VITA

Surname: Sasaki Given Names: Ryan Roe

Place of Birth: Halifax, Nova Scotia, Canada Date of Birth: April 30, 1977

Educational Institutions Attended

University of Prince Edward Island 1995-1999

Degree Awarded

B.Sc. University of Prince Edward Island 1999

Conference Presentation:

1. Ryan Sasaki and Peter Wan, Laser Flash Photolysis Study of the Photoarrangement of Dibenzo-*p*-dioxin. *85th CSC Conference,* Vancouver, BC, June 1-5, 2002.

Partial Copyright License

I hereby grant the right to lend my thesis (or dissertation) to users of the University of Victoria Library, and to make single copies only for such users or in response to a request from the Library of any other university, or similar institution on behalf or for one of its users. I further agree that permission for extensive copying of this thesis for scholarly purposes may be granted by me or a member of the University designated by me. It is understood that copying or publication of this thesis for financial gain shall not be allowed without my written premission.

Title of Thesis: A Laser Flash Photolysis Study of the Intramolecular Photoisomerization and Reduction of Dibenzo-*p*-dioxins

Author

Ryan Roe Sasaki

July 29, 2002